CHARLES UNIVESITY

Faculty of Science

Department of Zoology

Study programme: Biology

Branch of study: Protistology

Bc. Martina Kornalíková

Analyses of *Monocercomonoides* genome sizes, ploidies and karyotypes

Analýzy velikosti genomu, ploidie a karyotypu u kmenů *Monocercomonoides*

DIPLOMA THESIS

Supervisor: Doc. Mgr. Vladimír Hampl, PhD.

Prague, 2019

Declaration:

I declare that this thesis is my copyrighted work. All literature and other resources I used while processing are listed in bibliography and properly cited. The thesis was not misused for obtaining the same or different academic degree.

In Prague, 3.1.2019 Bc. Martina Kornalíková

Acknowledgement:

I would like to express my gratitude to my supervisor Doc. Mgr. Vladimír Hampl, PhD. for the useful comments and remarks and to Sebastian Cristian Treitli who led me in the lab and thanks to him I was able to finish this thesis. There is one big thank you for his time, patience and experience he passed to me. Furthermore, I would like to thank my whole family and especialy to my husband, who has supported me throughout the entire study.

Abstrakt

Oxymonády jsou skupinou bičíkatých prvoků, žijících v prostředí s nízkou koncentrací kyslíku. Obývají především střeva hmyzu a obratlovců. V této studii se zaměřujeme na analýzu ploidie a karyotypu různých druhů oxymonád pomocí metody fluorescence *in situ* hybridizace (FISH) s použitím prób proti jednokopiovým genům a telomerickým repeticím. Také jsme se pokusili odhadnout velikost genomu těchto druhů oxymonád pomocí průtokové cytometrie. S použitím specifických FISH prób proti SufDSU genu, který je pravděpodobně přítomenv jedné kopii v genomu, ukázali, že všechny studované kmeny jsou haploidní. Z genomu *Monocercomonoides exilis* víme, že oxymonády mají původní typ telomerické repetice (TTAGGG). Použitím próby proti těmto telomerickým repeticím jsme se pokusili odhadnout počet chromozomů u sedmi kmenů (pěti druhů) *Monocercomonoides*. Kromě jedné vyjímky byl průměrný počet signálů pod 20, což naznačuje počet chromozomů v řádu jednotek. V kmenech *M. mercovicensis* jsme ovšem zaznamenali mnohem vyšší počet signálů naznačujících, že buňky mají mnohem vyšší počty chromozomů. Nakonec jsme stanovili obsah DNA v jádreh těchto kmenů pomocí průtokové cytometrie se standardem *M. exilis* PA203, jehož velikost genomu je známa (82Mbp). Výsledky ukazují, že většina kmenů má menší velikost genomu podobnou nebo menší, než *M. exilis* PA203, naproti tomu druh *M. mercovicensis* má velikost genomu téměř 130 Mbp.

Klíčová slova: oxymonády, FISH, ploidie, karyotyp, obsah DNA, *Monocercomonoides*

Abstract

Oxymonads are a group of flagellate protists living in low oxygen environments - mainly the guts of insects and vertebrates. In this study, we focus on the analysis of ploidy and karyotype of various species of oxymonads using Fluorescence *In Situ* Hybridization (FISH) with probes against single copy genes and telomeric repeats as well as estimating the DNA content in the nuclei of these oxymonads using flow cytometry. Using specific FISH probes against SufDSU gene, which is present in a single copy in the haploid genome, we showed that all studied strains are probably haploid. From the genome of *Monocercomonoides exilis* strain PA203 we know that oxymonads have the ancestral type of telomeric repeat (TTAGGG). Using a probe against these repeats we tried to label chromosome ends and estimate the number of chromosomes for seven strains (five species) of *Monocercomonoides.* With a single exception, the average number of signals per nucleus was below 20 indicating number of chromosomes below 10. In the strains of *M. mercovicensis*, we observed much higher number of signals suggesting that the cells have much higher number of chromosomes. Finally, we established the DNA content for several strains using flow cytometry. We used as a standard *M. exilis* strain PA203 knowing that the haploid genome size is approximately 82Mbp. Results indicate that most of the strains have genomes smaller or similar to *M. exilis* except for *M. mercovicensis*, whose genome size is almost 130Mbp.

Key words: Oxymonads, FISH, ploidy, karyotype, DNA content, *Monocercomonoides*

List of abbreviations

AAD	Aminoactinomycin D
ADCs	Analog to digital convertors
AMP	Ampicilin
DAPI	4',6-diamidino-2-phenylindole
dNTP	Dinucleoside triphosphate
DNA	Deoxyribonucleic acid
DNaseI	Deoxyribonuclease I
DNP-11-dUTP	Dinitrophenol (DNP) labeled deoxyuridine triphosphate¨
dUTP	Deoxyuridine triphosphate
GSs	Genome size of the sample
GSr	Genome size of the reference
EM	Electron microscopy
FISH	Fluorescence in situ hybridization
FITC	Fluorescein isothiocyanate
FR	Fluorescence ratio
FSC	Forward scattered light
HRP	Horseradish peroxidase
LB	Lysogeny broth
LM	Light microscopy
PBS	Phosphate buffered saline
PI	Propidium iodide

PMTs	Photomultiplier tubes
RALS	Right-angle light scatter
RNA	Ribonucleic acid
RT	Room temperature
SOC	Super Optimal broth with Catabolite repression
SSC	Side scattered light
SSC based buffers	Saline sodium citrate
TG-1	Termite group 1
TRITC	Tetramethylrhodamine
TAE buffer	Tris-acetate-EDTA buffer
TSA	Tyramide signal amplification
7-AAD	7-aminoactinomycin D
90LS	90-degree light scatter

Table of Contents

1. Introduction

Oxymonads are a group of flagellates members of Metamonada (Excavata), where they are part of the clade Preaxostyla, together with genera *Trimastix* and *Paratrimastix*. Oxymonads live under anaerobic or microaerophilic conditions, usually in the gut of insects and vertebrates. Most oxymonads possess four flagella, one of which is recurent. One of the most interesting features of oxymonads is that they lost the mitochondrion and typical Golgi aparatus. Oxymonads are divided into five families, Polymastigidae, Saccinobaculidae, Pyrsonymphidae, Streblomastigidae and Oxymonadidae plus the isolated genus *Opisthomitus* sp. The phylogenetic relationships within oxymonads are not very well known.

Fluorescence in situ hibridization (FISH) is a technique which allows visualization, identification, enumeration and localization of specific nucleic acid (DNA or RNA) sequences by hybridizing fluorescently labelled probes to its complementary sequence on or outside chromosomes or in the RNA within cells previously fixed on slides. Usually the FISH protocols consist of six steps: (1) sample preparation, (2) fixation, (3) hybridization with labeled probe, (4) washing, (5) counterstaining and finally (6) visualization using fluorescence microscopy. The probe can be labeled directly or indirectly. We used indirect labeling with digoxygenin and detected it using anti-digoxygenin antibody conjugated with Dylight 488 (in case of telomeric repeats) or with HRP followed by tyramide signal amplification (in case of single copy genes).

Flow cytometry is a technology used for counting, sorting and profiling cells in a fluid mixture using optical and fluorescence characteristics of single cells. The flow cytometer consists of four systems: fluidics, optics, electronics, and computer interface.

The aim of this thesis was to analyse karyotypes of investigated strains of *Monocercomonoides* using FISH and to estimate the ploidy and genome size using single copy gene FISH and flow cytometry.

2. Theoretical part

2.1. Oxymonads

Oxymonads are a monophyletic group of heterotrofic flagellates which live under anaerobic or microaerophilic conditions (Keeling and Leander, 2003; Simpson et al., 2002; Treitli et al., 2018). The representatives of this group are morphologically well-defined protists, and a rather diverse lineage of eukaryotes (Moriya et al., 2003). Morphologically, they are very diversified, with extreme variations in cell size and shape, from the smallest flagellates of *Monocercomonoides* to the huge forms *Oxymonas* or *Pyrsonympha* (Moriya et al., 2003).

With the exception of *Monocercomonoides merkovicensis*, the members of this group are not free living (Treitli et al., 2018). Typically, they inhabit the guts of insects (Hampl, 2017; Keeling and Leander, 2003; Treitli et al., 2018), most representatives inhabiting the hindgut of lower termites and the gut of the wood-feeding cockroaches with the exception of several species of *Monocercomonoides* that occur also in guts of vertebrates (Hampl, 2017; Moriya et al., 2003; Treitli et al., 2018). Oxymonads feed by pinocytosis or phagocytosis, and they do not have a specialized cytostome (Treitli et al., 2018). The relationship between termites and these microorganisms is a great example of symbiosis. The small oxymonads do not ingest cellulose but feed by osmotrophy or by phagocytizing prokaryotes. Larger oxymonads are cellulose digesters (Dacks et al., 2001; Radek, 1994) with their bacterial ecto- and endosymbionts which are probably involved in the cellulose digestion process (Hampl, 2017).

Oxymonads ancestrally they possess four flagella, which are arranged in two pairs, and one of the flagella being recurrent. They have a karyomastigont which is formed by flagella, nucleus and two pairs of basal bodies which are connected by preaxostyle. A microtubular rod called axostyle runs through the whole length of the cell (Hampl, 2017; Radek, 1994; Radek et al., 2014).Trophozoites are the dominant life stages of the cell cycle (Hampl, 2017). Oxymonads divide by binary fission and closed mitosis with an intranuclear spindle (Hampl, 2017).The most anterior basal body (4) is associated with a microtubular root which underlies the microtubular sheet called pelta. Pelta and preaxostyle are partially covering the nucleus (Hampl, 2017). Depending on the genus of oxymonads they can have multiple karyomastigonts (Radek, 1994). Some oxymonads in the family Oxymonadidae have a

microfibrillar structure, called proboscis or „rostellum“, which is often situated in the anterior part of the cell and used to attachment to the intestinal wall (Hampl, 2017; Moriya et al., 2003).

Among common features in this group is the lack of mitochondria (Hampl, 2017; Karnkowska et al., 2016; Keeling and Leander, 2003), peroxosimes (Hampl, 2017), typical Golgi apparatus (Moriya et al., 1998), however, there are present genes which encode proteins functional in Golgi, indicating the existence of a cryptic Golgi (Karnkowska et al., 2016).

Most oxymonads have prokaryotic symbionts (Noda et al., 2006, 2003). They may possess bacteria of various morphologies attached as ectosymbionts on the surface of the protist cells (Leander and Keeling, 2004; Noda et al., 2006). The most common bacterial symbionts are spirochaetes which are the most common group of bacteria found in the gut of the termites (Noda et al., 2003) followed by bacteria belonging to order *Bacteroidales* or *Enterobacterales* (Noda et al., 2006). In addition to that, various types of bacteria are located inside the protist cell, surrounded by two membranes. These intracellular symbionts were identified as as "*Endomicrobium*" (TG-1) or methanoarchea (Stingl et al., 2005).

2.1.1. Oxymonad taxonomy

Oxymonads are members of Metamonada (Excavata) where they form a clade Preaxostyla (Simpson, 2003) together with the genus *Trimastix* and *Paratrimastix* (Dacks et al., 2001; Zhang et al., 2015). The relationships within oxymonads are not well known (Treitli et al., 2018). Potential evolution and diversity of Preaxostyla are shown in the Figure 1.

Many species have been described only by morphological features with more than 140 species being described to date (Hampl, 2017). There are five families of oxymonads (Moriya et al., 2003; Treitli et al., 2018) plus the isolated genus *Opisthomitus* sp. (Radek et al., 2014). Maximum likelihood tree of Oxymonadida, based on SSU rRNA gene sequences rooted with genera *Trimastix* and *Paratrimastix* is shown in Figure 2.

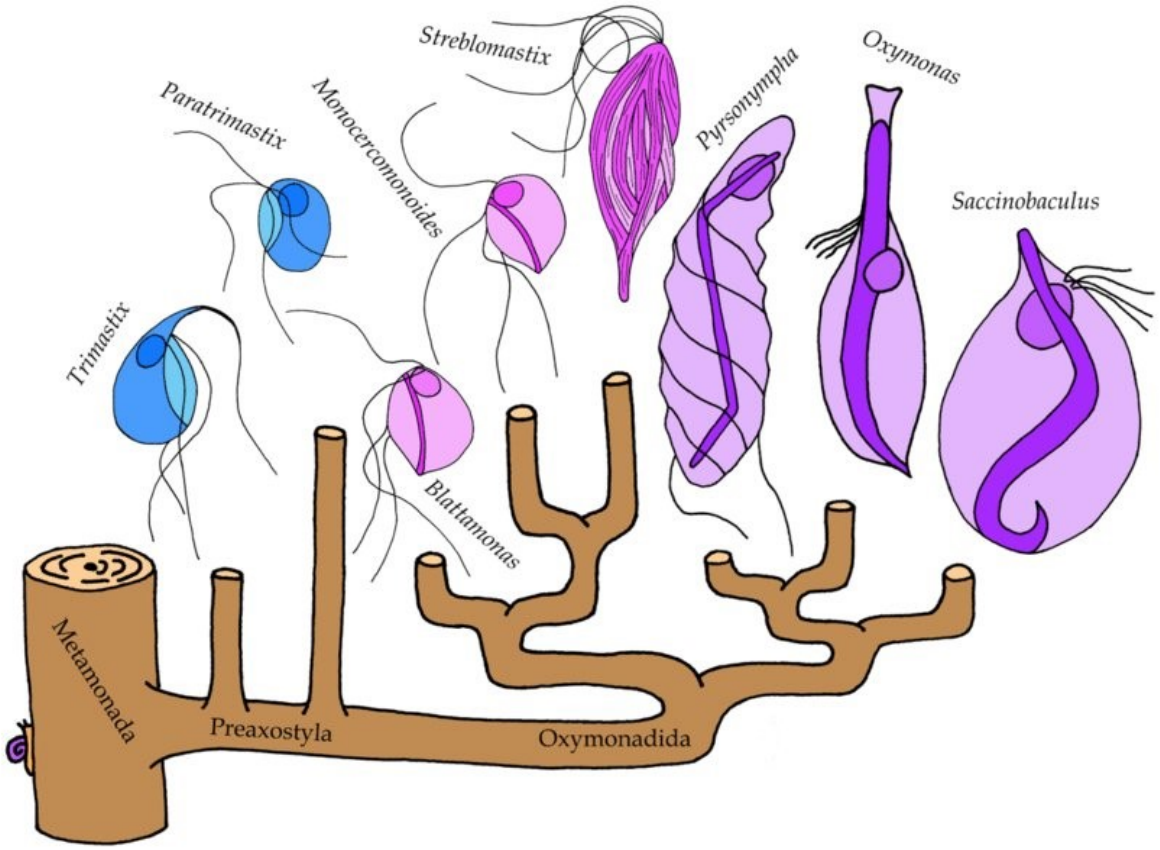

Figure 1: Schematic drawing of the evolution and diversity of Preaxostyla. With courtesy of LVF Novák (Unpublished).

2.1.1.1. Family Polymastigidae

Family Polymastigidae is a group of small oxymonads with four flagella, with at least one of the flagella being recurrent, pelta and axostyle are present, but attachment organelles are absent. The Polymastigidae family currently includes five genera: *Polymastix*, *Monocercomonoides*, *Blattamonas Tubulimonoides*, and *Paranotila*.

Genus *Monocercomonoides*

Monocercomonoides consists of small oval-shaped oxymonads with cells less than 20μm in length (Treitli et al., 2018), with four flagella arranged in two pairs separated by a preaxostyle, one flagellum is recurrent and partially attached to the cell (Hampl, 2017; Treitli et al., 2018) and with large nucleus covered by pelta (Brugerolle et al., 2003). About half of the representatives inhabit the digestive tract of wood-eating insect imagoes (the cockroaches *Cryptocercus* and lower termites), insect larvae (*Tipula*, Coleoptera) and the rest of the

species are found in the gut of vertebrates (rodents, bovids, reptiles, and amphibians) (Brugerolle et al., 2003; Hampl, 2017; Radek, 1994)

Genus *Blattamonas*

Blattamonas trophozoites are small oval-shaped cells with pointed posterior end, usually less than 10 µm in length. They possess four flagella, one of which is recurrent and usually does not adhere to the cell. The most notable difference from *Monocercomonoides* is that the axostyle is always protruded from the cell posterior and it is surrouned by periaxostylar ring (Treitli et al., 2018).

Genus *Tubulimonoides*

This genus is similar to *Monocercomonoides,* but the difference lies in its tubular axostyle. *Tubulimonoides* was described from the gut of *Gryllotalpa Africana* (Krishnamurthy and Sultana, 1976).

Genus *Polymastix*

Polymastix has spindle shaped cells which are around 10 µm in length, with four flagella, one of which is longer than the cell body. As opposed to the flagellar organization found in *Monocercomonoides*, there is no recurrent flagellum in *Polymastix*. The characteristic feature of *Polymastix* is the presence of long symbiotic fusiform bacteria on the surface. *Polymastix* species have been found in the hindgut of insects and myriapods. More than 11 species are described (Brugerolle et al., 2003; Hampl, 2017).

Genus *Paranotila* (Cleveland, 1966)

Only one species, *P. lata,* was described by Cleveland from the gut of *Cryptocercus punctulatus*. The cells are larger (15–25 µm) and they have a single nucleus and four flagella which are barely adhering to the cell (Hampl, 2017).

2.1.1.2. Family Streblomastigidae

This family contains one genus with only a single species *Streblomastix strix*, which was found in the hindgut of the damp-wood termites of the genus *Zootermopsis*. The cell is spindle-shaped, typically 15–50 µm long, but the cells can be larger. It has four flagella which are not adhering to the cell. On the anterior side of the cell there is a thin rostellum with a holdfast for attachment to the gut epithelium. The cell is covered by long rod-shaped epibiotic

bacteria closely related to genus *Bacteroides* (Hampl, 2017; Leander and Keeling, 2004; Noda et al., 2006).

2.1.1.3. Family Saccinobaculidae

Saccinobaculidae has representatives which are symbionts found in the hindgut of the wood-feeding cockroaches *Cryptocercus punctulatus* and *C. relictus*.

Genus *Saccinobaculus*

The mastigont consists of two pairs of basal bodies associated with a preaxostyle. Multiplication of flagella is associated with multiplication of preaxostyles and the nucleus is covered by a pelta. Epibiotic bacteria are rarely present. Seven species of *Saccinobaculus* are currently recognized (Carpenter et al., 2011; Hampl, 2017; Mcintosh, 1973; McIntosh et al., 1973).

Genus *Notila*

Notila has differences in sexual cycles compared to *Saccinobaculus*. The main difference is that both trophozoites and "gametes" of *Notila* are diploid. *Notila* differs morphologically from *Saccinobaculus* by its axostyle which does not protrude (Hampl, 2017).

2.1.1.4. Family Oxymonadide

All known species are symbionts in the hindgut of termites. To be able to attach to the intestinal wall, they have a microfibrillar structure, called „rostellum", which can be much longer than the cell. Epibiotic rod-shaped bacteria are densely covering the whole surface of the cell.

Oxymonas

Oxymonas has elongated ovoid cell body with the cell length between 5 and 240 µm and the width between 4 and 165 µm. Rodlike bacteria adhere to the surface. More than 30 species have been described (Brugerolle and König, 1997; Hampl, 2017; Rother et al., 1999).

Microrhopalodina (syn. *Proboscidiella*)

The ovoid or pear-like cell body of *Microrhopalodina* anteriorly elongates into a long and slender rostellum. The cell size varies from 23 to 165 µm in length and 11 to 113 µm in width and the cell has multiple karyomastigonts, their number can vary from four up to 50 and

they are located at the base of the rostellum in a collar. The surface of the cell is covered by external surface structures and rod-like bacteria. Four species have been described (Hampl, 2017; Rother et al., 1999).

Barroella (syn. *Kirbyella*)

Only two species have been described with the cell size between 27 and 224 µm in length and 11 to 80 µm in width. (Hampl, 2017).

Sauromonas

Sauromonas m'baikiensis, is the only species of the genus, and it is a symbiont of the termite *Glyptotermes boukoko*. (Hampl, 2017).

2.1.1.5. Family Pyrsonimhydae

The family contains 25 described species in two genera and all of them are symbionts of the lower termites from genus *Reticulitermes*. On the surface of the cells they can have epibiotic bacteria and most of the species have endobiotic bacteria in the cytosol (Hampl, 2017; Hongoh et al., 2007; Iida et al., 2000; Yang et al., 2005).

Genus *Pyrsonympha*

Pyrsonympha has large cells with 100-150 µm in length and 30-40 µm in width. On the posterior part of cell there is often a holdfast. The surface of the cell is usually covered with ectosymbiotic spirochaetes. This genus contains 13 described species (Hampl, 2017; Hongoh et al., 2007; Iida et al., 2000; Stingl et al., 2005; Yang et al., 2005).

Genus *Dinenympha*

Cells of *Dinenympha* are smaller with four flagella. They are inhabiting the hindgut of lower-termites. There was a long-lasting debate about *Pyrsonympha* and *Dinenympha* that they don't represent different genera but they are different morphotypes of the same species, which was apparently resolved by molecular studies showing that they do not contain the same SSU rDNA sequence. The *Pyrsonympha* and *Dinenympha* clades are strongly supported as separate clades. To date 12 species have been described (Hampl, 2017; Iida et al., 2000; Moriya et al., 2003).

2.1.1.6. Opisthomitus

Genus *Opisthomitus*

Opisthomitus is a small oxymonad with an average length of 9.6 µm (7–13 µm) and an average width of 2.8 µm having four flagella which are 4–5 times longer than the cell body. *Opisthomitus* is morphologically similar to *Monocercomonoides*, as it possesses pelta, which is supported by a microtubular root associated with anterior basal body 4. The genus contains two species *Opisthomitus avicularis* and *O. longiflagellatus*, and two species with uncertain phylogenetic position, *O. brasiliensis* and *O. flagellae*. The genus is not classified into any oxymonad family, but based on the 18S rRNA phylogeny it seems like it is closely associated with the family Pyrsonymphidae (Hampl, 2017; Radek et al., 2014).

Figure 2: Maximum likelihood tree of Oxymonadida, based on SSU rRNA gene sequences rooted with genera *Trimastix* and *Paratrimastix*. Names in the brackets represent host species and icons represent the host main group. Scale bar corresponds to 0.04 expected substitutions per site (Treitli et al., 2018).

2.2. Flourescence *in situ* hybridization

2.2.1. Short introduction and history

Fluorescence *in situ* hybridization (FISH) is a cytogenetic technique which was developed in the early 1980s (Hu et al., 2014) as a physical mapping tool to sketch genes on chromosomes (Cui et al., 2016). The earliest *in situ* hybridizations using radioisotopic probes (Levsky and Singer, 2003) were performed on *Xenopus* oocytes and detected by microautoradiography (Moter and Göbel, 2000) in a study published by Pardue and Gall in 1969 (Clark, 2002).

The first use of FISH in bacteriology was done by Giovannoni with radiolabeled probes specifically hybridized to unique domains of 16S rRNA sequences from bacteria (Giovannoni et al., 1988). However, the use of radiolabeled probes had some drawbacks, mainly because the specific activity of probes was not constant and needed to be recorded on radiography film, the need for long exposure time which extends the experiment duration and of course radiolabeled probes are expensive and dangerous (Levsky and Singer, 2003). Therefore radiolabeled probes were replaced with non-isotopic dyes which are safer and provide better results (Moter and Göbel, 2000). The first application of fluorescent *in situ* detection was reported in 1980 (Bauman et al., 1980; Levsky and Singer, 2003). In 1982, the first DNA probes labeled with biotin were developed and detected with antibodies conjugated to fluorescent or enzymatic reagents (Manuelidis et al., 1982). In early 1990s, the first specific deoxyoligonucleotide probes conjugated with fluorochromes were synthesized which allowed the direct detection (Kislauskis et al., 1993). Although the number of FISH detection methods have increased significantly, and the target types have become quite varied, the main principles of FISH remained the same.

Nowadays the FISH technique is used for visualization, identification, enumeration and localization of specific nucleic acid (DNA or RNA) sequences by hybridizing fluorescently labelled probes to its complementary sequence on chromosomal preparations or whole cells peviously fixed on slides (Hu et al., 2014; Moter and Göbel, 2000; Shah et al., 2015; Volpi and Bridger, 2008). Probes are labeled directly, by incorporation of fluorescent nucleotides, or indirectly, by incorporation of nucleotides labeled with reporter molecules that are afterwards detected by fluorescent antibodies. Probes and targets are finally visualized *in situ* by fluorescent microscopy (Volpi and Bridger, 2008). Compared to the conventional cytogenetic metaphase karyotype analysis, FISH does not need cell culturing, and can directly

use fresh or paraffin-embedded interphase nuclei for a rapid detection (Hu et al., 2014). FISH is usually used for detecting of chromosomal aberrations, aneuploidies, microdeletion or microduplication syndromes, and subtelomeric rearrangements (Cui et al., 2016; Hu et al., 2014). FISH is able to identify chromosomal rearrangements in around 80% of the cases, while conventional cytogenetic techniques can identify chromosomal aberrations in only 40-50% of the cases (Hu et al., 2014). FISH is also used for detecting malaria infection in blood smears (Shah et al., 2015) or genetic diseases, hematologic malignancies, and solid tumors (Cui et al., 2016; Hu et al., 2014). FISH is being increasingly used in clinical genetics, neuroscience, reproductive medicine, toxicology, microbial ecology, evolutionary biology, comparative genomics, cellular genomics, and chromosome biology (Giovannoni et al., 1988; Volpi and Bridger, 2008).

FISH tests are highly reproducible with high resolution to a single gene level with high sensitivity and specificity (Cui et al., 2016; Shah et al., 2015) and offers advantage of direct application on both metaphase chromosomes and interphase nuclei, and visualization of hybridization signals at the single-cell level (Cui et al., 2016).

2.2.2. FISH principle

Usually FISH assays consist of six steps: (1) sample preparation, where the cells are subjected to a hypotonic shock before fixation in combination with dropping of the cells on glass slides followed by air drying of the slides, (2) fixation of the sample, followed by permeabilization of the cell walls and membranes using enzymes or detergents which is necessary to facilitate entry of the probes or detection reagents, (3) hybridization to promote duplex formation between labelled probe and the target, (4) washing, to remove unbound probes, (5) counterstaining and mounting, and finally (6) visualization by fluorescence microscopy (Amann et al., 2001; Hepperger et al., 2007; Moter and Göbel, 2000; Shah et al., 2015; Spear et al., 1999; Volpi and Bridger, 2008). Basic steps of FISH are shown on the Figure 3.

2.2.2.1. Sample preparation

During the sample preparation the cells are usually subjected to a hypotonic shock. Hypothonization is performed to swell the cells and nuclei before fixation (Moter and Göbel, 2000). After hypotonization the cells can be either fixed immediately or can be attached to glass slides then air dried followed by fixation (Moter and Göbel, 2000). For good attachment of samples on glass slides it is good to treat the surface of the slides with coating agents (e.g. gelatin, poly-L-lysine).

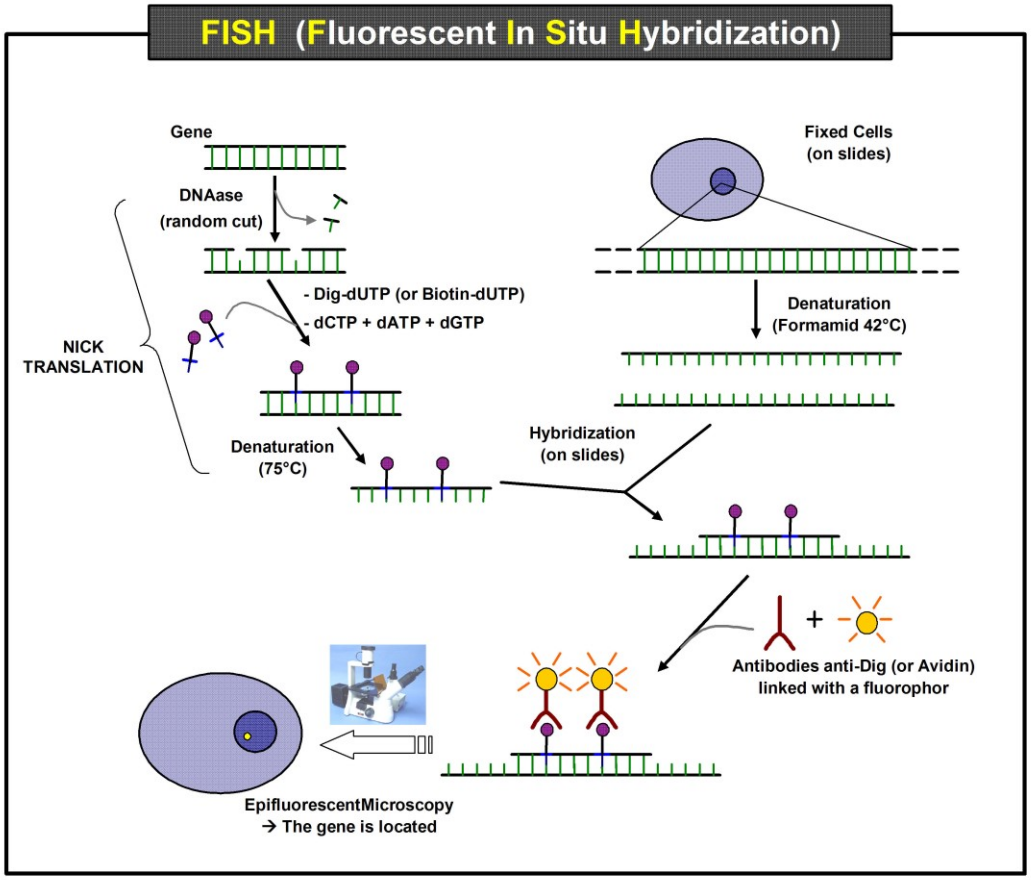

Figure 3: Basic steps of fluorescence in situ hybridization (**https://www.creative-biolabs.com/fluorescent-in-situ-hybridization-FISH.html**)

2.2.2.2. Fixation

There are two categories of fixatives, cross-linking agents (e.g. formaldehyde, glutaraldehyde, acrolein, osmium tetroxide) – these fixatives form cross-linkage with their targets and precipitating agents (e.g. methanol, ethanol) – these fixatives coagulate and/or precipitate proteins, but do not fix carbohydrates and lipids and are used only for light microscopy (M. Kuwajima, 2011). Generally, the fixation conditions should preserve the cell

integrity and it should have minimal impact on fluorescence. It is always important to think about the type of sample and the type of fixation which will be used in order to have the optimal fixation which will provide a good probe penetration, retention of the target RNA or DNA while maintaining the cell integrity and morphology. (Moter and Göbel, 2000; Spear et al., 1999).

2.2.2.3. Hybridization and stringency washes

First, the probes and nucleic acids together with fixed and permeabilized cells or chromosomal spreads are denaturated (Nedbal et al., 2012), then hybridization must be done under strict conditions for correct annealing of fluorescent-labeled probe and the target DNA or RNA sequences. The hybridization mixture must contain certain concentration of formamide which acts as a destabilizer by lowering the melting temperature of hybrids, thus increasing the stringency of the probe to target binding. Optimal concentration of formamide together with strict hybridization temperatures will result in minimal nonspecific hybridization. For DNA FISH, the hybridization is performed usually overnight in a dark humid chamber at 37 ^{o}C. For RNA FISH, the hybridization time can be shortened.

Afer hybridization, post hybridization washes are necessary to remove nonspecific interactions between the probe and undesirable regions of the genome, which increases the probe specifity. Usually the first washes also use formamide to destibilize the double strands, then the buffers used in post-hybridization washing are SSC based and therefore provide positively charged sodium ions in solution. However, using too high concentration of SSC in the washing buffer will produce a poor washing effect with low stringency and too little SSC (or just water) will tend to wash all the probe away from the sample due to high stringency. Temperature and pH also influence the washing effect; increasing the temperature increases the stringency and the pH determines the availability of the positive ions. The inclusion of TWEEN 20 detergent decreases background staining and enhances the spreading of the reagents in the wash buffers (Chen and Chen, 2013; Connolly et al., 2002; Moter and Göbel, 2000).

2.2.2.4. Counterstraining

Counterstraining and mounting of all stained biological samples is an important step before the microscopic analysis. Mounting enables the slides to be archived for long periods of time. Counterstaining aids in visualization and localization of targets, facilitating

interpretation of morphology and cell structure within the samples of interest (Rieder et al., 2011; Wilder, 1935).

Usually FISH samples are counterstained with fluorescent agents which stain DNA. The most often used counterstain is DAPI. DAPI is a fluorescent dye which strongly binds A-T rich regions in DNA and is usually used to stain cell nuclei or chromosomes. DAPI has an absorption maximum at around 358 nm and an emission maximum at 461 nm (Kapuscinski, 1995).

2.2.2.5. Microscopy analysis

Microscopic analysis can be done using epifluorescence microscope or confocal laser scanning microscope. Confocal microscopy has the advantage that can restrict the collected signal to a thin section of the investigated object, thus out of focus fluorescence is removed which is leads to more sharp images (Moter and Göbel, 2000).

2.2.3 Probe labeling and synthesis

One of the most critical steps in FISH is the probe design. Probes used for single-copy targets are typically short fragments derived from the target sequence with known sequence. FISH on repetitive targets such as chromosomal satellites or telomere repeats can be detected with conventional DNA probes or labeled oligonucleotides (Nedbal et al., 2012).

DNA probe labeling can be performed by (1) direct labeling using PCR, (2) direct labeling of the oligonucleotides, (3) nick translation or (4) random primer labeling method. (Feinberg and Vogelstein, 1983; Morrison et al., 2002). Different types of labeling are illustrated in the Figure 4.

The probe labeling can be done directly or indirectly as showed in Figure 5. In the case of direct labeling, a fluorescent dye is directly bound to an oligonucleotide either chemically in the course of synthesis using the aminolinker at the 5′ end of the probe (Figure 4a) or enzymatically when the fluorescently labeled nucleotides are attached to the 3′end using terminal transferase (Figure 4b) or using random priming method. Direct labelling is used more often because it is faster, cheaper and it does not require any other steps after hybridization, because direct labeled probes can be visualized after post-hybridization washes, which reduces the processing time significantly. But in this case the signal strength is usually only 10-15% of that what can be produced by indirect labeling (see below). Also, directly

labeled probes are prone to photobleaching during preparation and hybridization, so it is necessary to avoid exposure to strong light.

In indirect labeling a hapten molecule is used, like for example digoxygenin or biotin, which is later detected immunohistochemically by a fluorophore-tagged antibody (Figure 4c). Indirect labeling can create better fluorescence signal, but it extends significantly the protocol duration. Biotin, also known as vitamin H, is detected by streptavidin. But it can happen that endogenous biotin from biological samples often interferes with biotin detection resulting in high backgrounds and false positives. The digoxigenin is a steroid present in *Digitalis* plants and it is detected by digoxigenin antibody conjugated with a fluorescent dye or a reporter enzyme. In the latter case, the nucleotides are labeled with digoxygenin and the antibody is labeled usually with horseradish peroxidase (HRP) that can use fluorescein-tyramide as substate for catalized deposition and signal amplification (Figure 4d).

Typical oligonucleotide probes are between 15 and 30 bp in length. Shorter probes should have easier entry to their targets, but there is possibility that they will not be able to carry enough labels for the signal to be detected. Indirect labeling works better in these situations and it used for very small genomic targets because of its potential to increase signal intensity (Chen and Chen, 2013; Morrison et al., 2002; Moter and Göbel, 2000; Ratan et al., 2017; Sharpe et al., 2002; Spear et al., 1999).

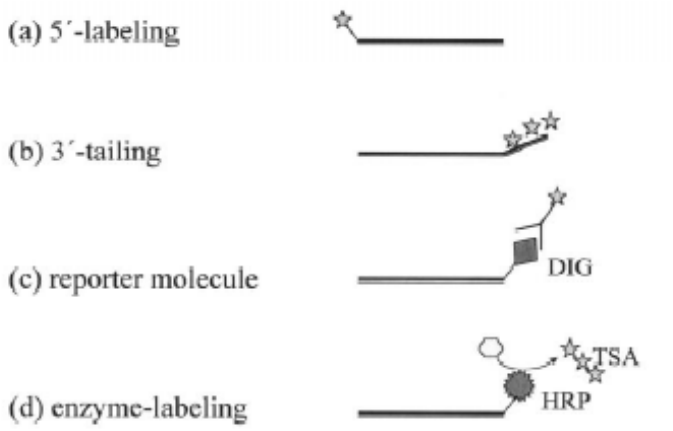

Figure 4: Probe Labeling: Direct labeling of the probes is illustrated in (a) and (b). Indirect probe labeling with detection using fluorescently labeled antibody is illustrated in (c) and labeling of the probes using horseradish peroxidase (HRP) followed by Tyramide Signal Amplification (TSA) is illustrated in (d) (Moter & Göbel, 2000).

Depending on the regions of interest and labeling type, the probes can be locus-specific which target specific regions or genes or the probes can be regional painting ones which are used for specific chromosomal bandings, detection of an entire chromosome or even whole genome (Cui et al., 2016).

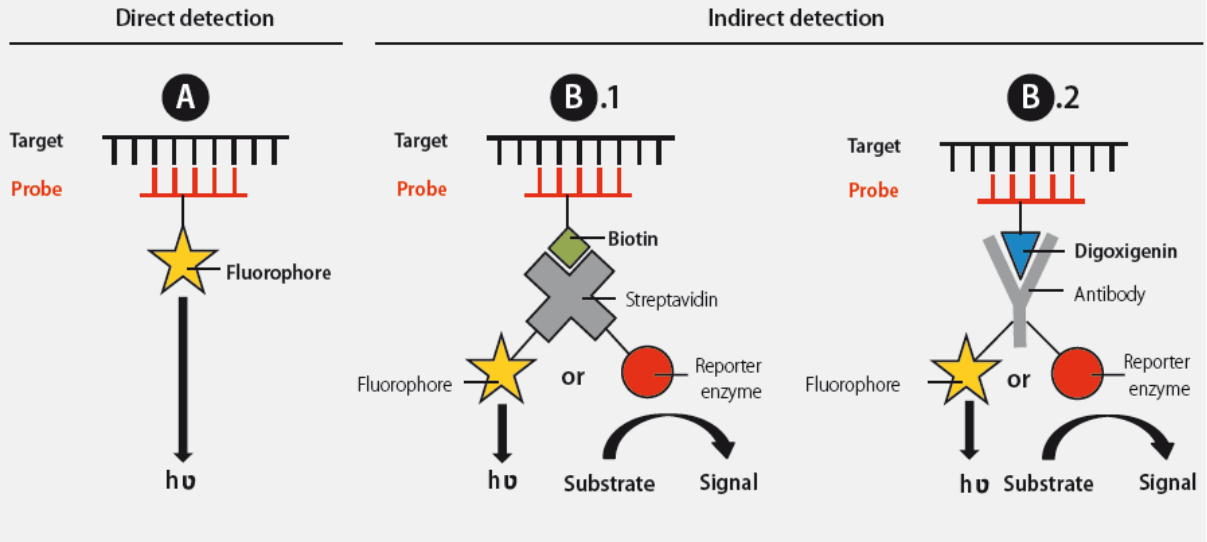

Figure 5: Direct and indirect labeling probes. Fluorescently labeled probes can be detected directly after incorporation (A) whereas indirect detection via Biotin/Streptavidin (B.1) or Digoxigenin/Antibody (B.2) systems offers possibility for signal amplification and increased stability (https://www.jenabioscience.com/images/741d0cd7d0/Non_radioactive_Labeling_DNA_RNA_web.pdf).

2.2.3.1. Oligonucleotide labeling

Direct labeling of oligonucleotides is a method in which a stable bond is formed between the nucleic acid and the fluorophore complex. The oligonucleotides are synthesized with primary amino group at the 5′end. The fluorescent dyes are coupled to these amino groups, and the dye-oligonucleotide conjugates are created (Morrison et al., 2002; Wallner et al., 1993).

2.2.3.2. Direct incorporation by PCR

Direct incorporation by PCR is one-step labeling of the probes using polymerases to incorporate labeled nucleotides. In this case the fluorophores are already attached to nucleoside triphosphates which are then incorporated into the probe by the polymerase (Morrison et al., 2002).

2.2.3.3. Nick translation

Nick translation is a method where labeled nucleotides are incorporated into DNA using of a combination of two enzymes, deoxyribonuclease I (DNase I) which nicks the DNA, and DNA polymerase I, which is adding nucleotides starting from the nick location. The 5' to 3' exonuclease activity of the polymerase removes nucleotides from the 5' end of the nick as the polymerization proceeds. In the end there is no net synthesis of DNA and during the reaction various length fragments of labeled and unlabled DNA are generated. The resultant double-stranded fragments must be denatured prior to hybridization (Morrison et al., 2002)..

2.2.3.4. Random primer labeling

Random primer labeling is a method where labeled nucleotides are incorporated along the length of a DNA fragment. The random primer mixture is usually made of hexamers, octamers, or decamers and this mixture is mixed with the DNA which should be labeled, and denatured. After denaturation, the small oligonucleotides anneal to the target DNA and act as primers which are extended using labeled and unlabeled nucleotides by the Klenow fragment of the DNA polymerase I. The labeled material must be denatured prior to hybridization (Feinberg and Vogelstein, 1983; Morrison et al., 2002)..

2.2.4. Type of labels

2.2.4.1. Direct labels

In this case, the fluorescent dyes are attached to the DNA directly, and no antibody is used. The most often used fluorophores for FISH include coumarins, fluorescein derivates (fluorescein isothiocyanate, FITC), rhodamine derivates (tetramethyl rhodamine isothiocyanate, TRITC, Texas red) and cyanine dyes like Cy3 and Cy5. The structures of these fluorophores are shown in Fig. 5 (Amann et al., 2001; Morrison et al., 2002; Moter and Göbel, 2000). Chemical structures of four common fluorophore classes are shown in the Figure 6 (A–D).

2.2.4.2. Indirect labels

Most used indirect labels are haptens, which are small molecules that triger a strong immune response (Erkes and Selvan, 2014). Probes can be labelled with biotin 1-dUTP, digoxigenin 1-dUTP or fluorescein 1-dUTP (Wiegant et al., 1991). Biotin (vitamin H) can be detected using fluorescent or enzymatic conjugates of streptavidin. The interaction between

biotin and streptavidin has one of the highest binding constants known (Langer et al., 1981). Digoxigenin is derived from a plant steroid hormone (Hart and Basu, 2009). The digoxin structure is composed of hydrophilic sugar unit and a hydrophobic steroid unit (Shreder, 2000). Digoxigenin it is usually detected using anti digoxigenin antibodies conjugated with fluorophores or reporter enzymes. Chemical structures of biotin and digoxigenin are shown at the Figure 6 (E, F).

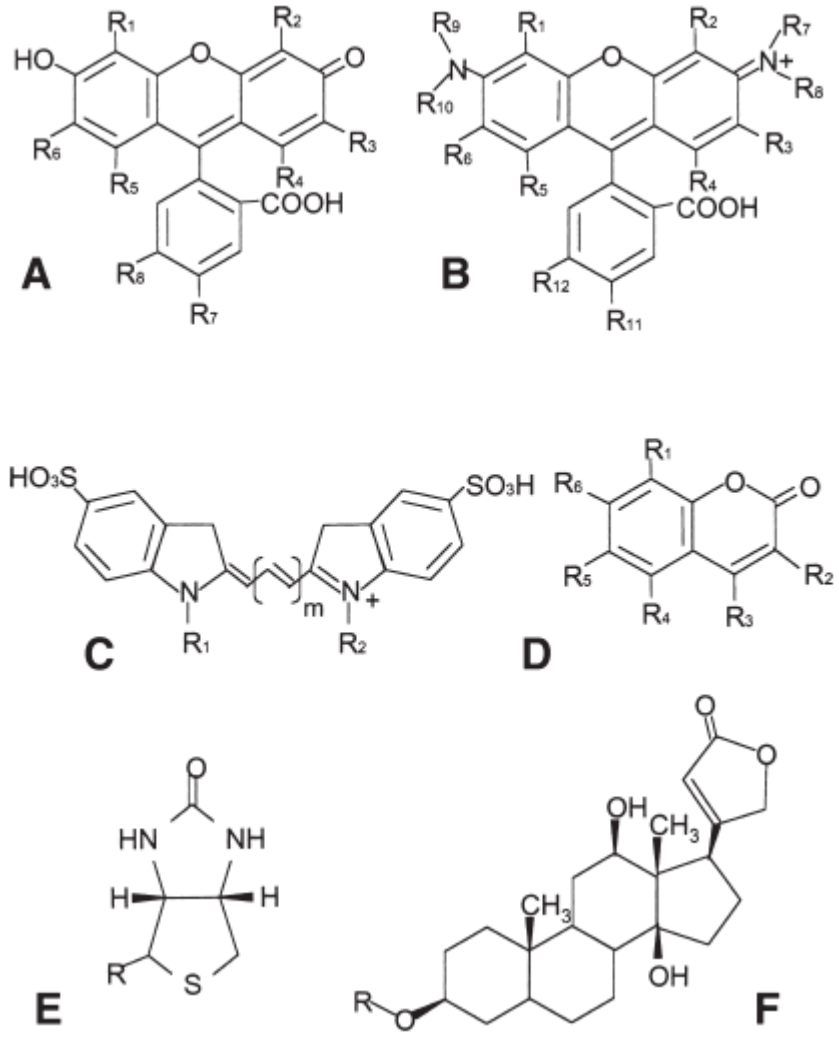

Figure 6: Chemical structures of four common fluorophore classes (A–D) and two common indirect labels (E and F). A. fluoresceins, B. rhodamines, C. cyanines (Cy 3, Cy 5, and Cy 7 only), D. coumarins, E. biotin, F. digoxigenin. Specific compounds in each class differ by their chemical substituents, indicated as R's in the chemical structures (Morrison et al., 2002).

2.2.5. Probe detection

2.2.5.1. Direct detection

Directly labeled probes can be visualized after post-hybridization washes, there is no needed any antibody detection.

2.2.5.2. Indirect detection

For indirect labelled probes, usually secondary reagents are used for detection. In indirect labeled probes with a hapten molecule like digoxygenin or biotin, they are detected with fluorescently labeled antibodies or antibodies labeled with horseradish peroxidase (HRP) which can later catalyze the deposition of soluble fluorophore at the site of detection.

2.2.5.2.1. Fluorescently labeled antibody detection

Hapten molecules present in labeled probes are detected immunohistochemically by a fluorophore-tagged antibody. Biotin can be detected using anti-biotin antibody conjugated with a fluorophore but more often biotin is detected using conjugated streptavidin. The digoxigenin is detected by anti-digoxigenin antibody conjugates with a fluorescent dye (Morrison et al., 2002).

2.2.5.2.2. Catalyzed reporter deposition

The tyramide signal amplification (TSA-FISH) it is based on enzymatic deposition of fluorochrome-conjugated tyramide by a reporter enzyme conjugated to an antibody or streptavidin (Khrustaleva and Kik, 2001). TSA-FISH is a multi-step procedure involving detection of a hybridized target with streptavidin-horseradish peroxidase or in case of digoxygenin with anti-digoxygenin conjugated with HRP followed by signal amplification, detection of amplified signal and imaging (Schriml et al., 1999). With TSA-FISH the detection sensitivity can be increased up to 100 times compared other existing techniques. HRP reacts with hydrogen peroxide and the phenolic part of labelled tyramide to produce aquinone-like structure bearing a radical on the C2 group. This ‘activated’ tyramide then covalently binds to tyrosine residues in close vicinity of the HRP, thus depositing many labelled tyramides closely to the probe that carries the HRP reporter (Khrustaleva and Kik, 2001; Raap, 1998; Schriml et al., 1999).

2.2.6. FISH limitations

There are several critical factors like hypotonic treatment, alcohol exposure time, duration of chemical and thermal denaturation, reagents like formamide which can lead to dilatation or attrition of the tissues and cells, strongly influencing chromatin morphology. Hypotonic treatment can also lead to an extension of the intracellular spaces. Dehydration leads to a considerable attrition of about 15–20% of the natural volume. The denaturation step of the target DNA is the most damaging step in the course of the FISH assays (Schwarz-Finsterle et al., 2007).

Another limitation of FISH comes from autofluorescence of microorganisms themselves or the autofluorescence of materials which are surrounding them which can decrease the signal to noise ratio and disguise the fluorescent signals. It can also happen that the probes will not shine strong enough or the signal intensity will be low because of the insufficient probe penetration for example in case of organisms with cell walls. Another problem can be photobleaching (Moter and Göbel, 2000).

2.2.7. Utilization of FISH techniques in karyotype and ploidy studies

2.2.7.1. Karyotype analyses using FISH

Telomeres are essential structures of eukaryotic chromosomes. Telomeres are located at the ends of eukaryotic chromosomes and they are composed of tandemly arranged short simple sequence repeats. The form TTAGGG is the telomeric repeat which occurs in rotest and fungi and seems to be the ancestral type of telomeric repeat (Alverca et al., 2007; Fulnečková et al., 2013).

Detection of telomeric sequences by FISH can be done using oligonucleotide probes which should show signals on the interphase nuclei or metaphase chromosomes (Sakai et al., 2007). Chromosome identification by FISH against the telomeric repeats can be used for example when the karyotype of chromosomes is difficult or impossible to assess using classic cytogenic techniques (Rae Rho et al., 2012; Silva et al., 2018).

FISH against telomeric repeats was used for various protists. For example, in the case of *Giardia intestinalis*, the telomeres were detected using specific probes prepared by PCR (Uzlíková et al., 2017). The probe was prepared using PCR with the forward $(TAGGG)_5$ and reverse $(CCCTA)_5$ primers which served both as primers and as templates for primer dimer extension. Labeling was done by random priming using digoxigenin and detected by anti-

digoxigenin antibody conjugated to horseradish peroxidase followed by tyramide signal amplification. The FISH signal number varied in cells depending on the cell cycle phase (Uzlíková et al., 2017).

Similar studies were also done on other protists like *Prorocentrum micans* and *Amphidinium carterae* where the probe was designed against the TTTAGGG repeats of the telomere and labeled with digoxigenin and detected with anti-digoxigenin antibody conjugated with FITC showing the signals exclusively at the chromosome ends (Alverca et al., 2007).

Karyotype analyses were also performed for *Chromera velia*. The telomere probe $(TTTAGGG)_4$ was used to examine the total number of chromosomes. The probe was labeled with dinitrophenol-11-2′-deoxyuridine 5′ triphosphate (DNP-11-dUTP) using the nick translation and detected by anti-DNP conjugated with HRP and TSA system was applied. The results suggested presence of four chromosomes (Vazač et al., 2018).

2.2.7.2. Ploidy analyses using FISH

To analyze the ploidy of an organism, usually a specific target is used which is well-known to be in a single copy per haploid genome. In this case, the method of choice is usually TSA-FISH. TSA-FISH was successfully used for detection single copy genes in plants (Khrustaleva and Kik, 2001; Pérez et al., 2009; Wang et al., 2006), humans (Schriml et al., 1999; Van Tine et al., 2004), animals, (Schriml et al., 1999; Van De Corput et al., 1998) rotest (Conrad et al., 2011; Vazač et al., 2018; Zubáčová et al., 2011), insects (Carabajal Paladino et al., 2014) or bacteria (Kawakami et al., 2010).

For example, TSA-FISH was used to study the ploidy in the human parasite *Trichomonas vaginalis* using probe against single copy genes. In this study the coding sequences of asparaginase-like threonine peptidase, acetylornithine amino- transferase, putative serine palmitoyltransferase and tryptophanase were used as probes. The probes were labeled by digoxigenin and detected using TSA with anti-digoxigenin antibody conjugated with HRP (Zubáčová et al., 2011). Also, the ploidy of *C. velia* was determined using TSA-FISH using probes for three different single copy genes. The probes were labeled with dinitrophenol-11-2′-deoxyuridine 5′ triphosphate (DNP-11-dUTP) and detected by anti-DNP conjugated with HRP and TSA system was applied. Resulting single signal from the cell indicated that cells are haploid (Vazač et al., 2018).

FISH using single copy genes was also used for the human parasite *Giardia intestinalis* (Tůmová et al., 2016). In this case, single color FISH was used where the probes were labeled with digoxigenin using random priming and detected using anti-digoxigenin conjugated with HRP and TSA system. Moreover, for *Giardia intestinalis* two-color FISH was also used with a combination of (1) a dig-labeled probe, anti-dig-HRP antibody, and TSA-Plus TMR and (2) a biotin-labeled probe, streptavidin-HRP, and TSA-Plus Fluorescein. The results showed that the *Giardia* cells are constitutively aneuploid (Tůmová et al., 2016).

2.3. Flow cytometry

Flow-cytometry is a fast, highly sensitive technique, which can quantitatively monitor many cell functions using a technology based on laser for counting, sorting and profiling of the cells in a fluid mixture (Fleck et al., 2006). The advantage of flow cytometry is that in a short time we can analyze large numbers of cells. Flow cytometry can measure optical and fluorescence characteristics of single cells (Brown and Wittwer, 2000; Trask et al., 1982). The flow cytometer consists of four main systems: fluidics, optics, electronics, and computer interface (Betters, 2015). The original flow cytometer was the Coulter counter invented by Wallace Coulter in the 1950s (Bakke, 2001).

2.3.1. Pricipes of flow cytometry

The flow cytometer as an instrument which consist of a fluidics system where the fluid sample is injected, an optics system which is used to illuminate the sample stream and detect the light signals and the electronics system which converts the light signals to data that can be visualized and interpreted by software (Bakke, 2001).

Flow cytometer uses the resistance of a cell in an electrical stream as it passes through a slot to resolve the number and the size of particle (Bakke, 2001). Cells in suspension are going through narrow fluid stream which allows the cells to go through individually (Brown and Wittwer, 2000; Olson et al., 1983). The cells are passed through a beam of monochromatic light, usually from a laser. When the particles from the sample stream pass through the laser beam, the light is scattered in all directions and is collected via optics through the filters and dichroic mirrors that isolate particular wavelengths. Some key parameters which are measured by the machine include forward light scatter (FSC), side light scatter (SSC), and fluorescence emission signals. Forward scattered light (FSC) is the light that is refracted by a cell in the forward direction and continues in the same direction and it is

proportional with the cell diameter. Usually, bigger particles produce more forward scattered light than smaller ones, and larger cells will have a stronger forward scatter signal. The light is also reflected by the cell and the cell internal structures. This is termed *side scatter* (SSC), *right-angle light scatter* (RALS), or *90- degree light scatter* (90LS). Side scattered light (SSC) is the light that is refracted by cells and travels in a different direction than its original course (measured at a 90° angle to the excitation line). It usually provides information about the granularity and complexity of the cells. Cells with a low granularity and complexity will produce less side scattered light and highly granular cells with a high degree of internal complexity will result in a higher side scatter signal (Bakke, 2001; Brown and Wittwer, 2000).

Fluorescence detectors measure the fluorescence signal intensity emitted from the cells. Within the flow cytometer, all these different light signals are split into defined wavelengths and channeled by a set of filters and mirrors in sucha a way that each sensor will detect fluorescence only at a specified wavelength. The signals are detected either using photodiodes or by photomultiplier tubes (PMTs) which converts the light signal into an electrical signal. Photodiodes are usually used to measure forward scatter when the signal is strong. PMTs are more sensitive instruments and are ideal for scatter and fluorescence readings. When light hits a photodetector, a small current is generated. Its associated voltage has an amplitude proportional to the total number of light photons received by the detector. This voltage is then amplified by a series of linear or logarithmic amplifiers, and by analog to digital convertors (ADCs), into electrical signals large enough (5–10 volts) to be plotted graphically. The amplification of the initial signal can be either linear or logarithmic. Linear amplification provides a direct visual relationship and is useful for scatter signals and fluorescent measurements of DNA. Logarithmic amplification is used for most other biologic signals, including immunofluorescence, mainly because of the extreme dynamic range of these signals.

The resulting data are represented as a 1-parameter histogram of the measured parameters for a cell population, described either as the percentage of cells within a set of markers or as the mean fluorescence intensity of a population, or two-dimensional dot-plot formats usually divided into four quadrants, each containing a percentage of the total population. 1-parameter histogram plots use typically the Y-axis as the number of events (the cell count) that show a given fluorescence, and the X-axis as the relative fluorescence intensity detected in a single channel. A large number of events detected at one particular

intensity will be represented as a peak on the histogram. Schematic overview of a typical flow cytometry is shown at Figure 7.

For analyzing data from the flow cytometry, it is important to selectively visualize the cells of interest and eliminate dead cells and debris. This strategy is called gating and it should contain the minimal or maximal gating boundaries to minimize data variability. It is important to have gating setting consistently during the course of the experiment to minimize data variability and to prevent conscious or unconscious data manipulation. (Bakke, 2001; Brown and Wittwer, 2000; der Strate et al., 2017; Olson et al., 1983; Rahman, 2014; Trask et al., 1982).

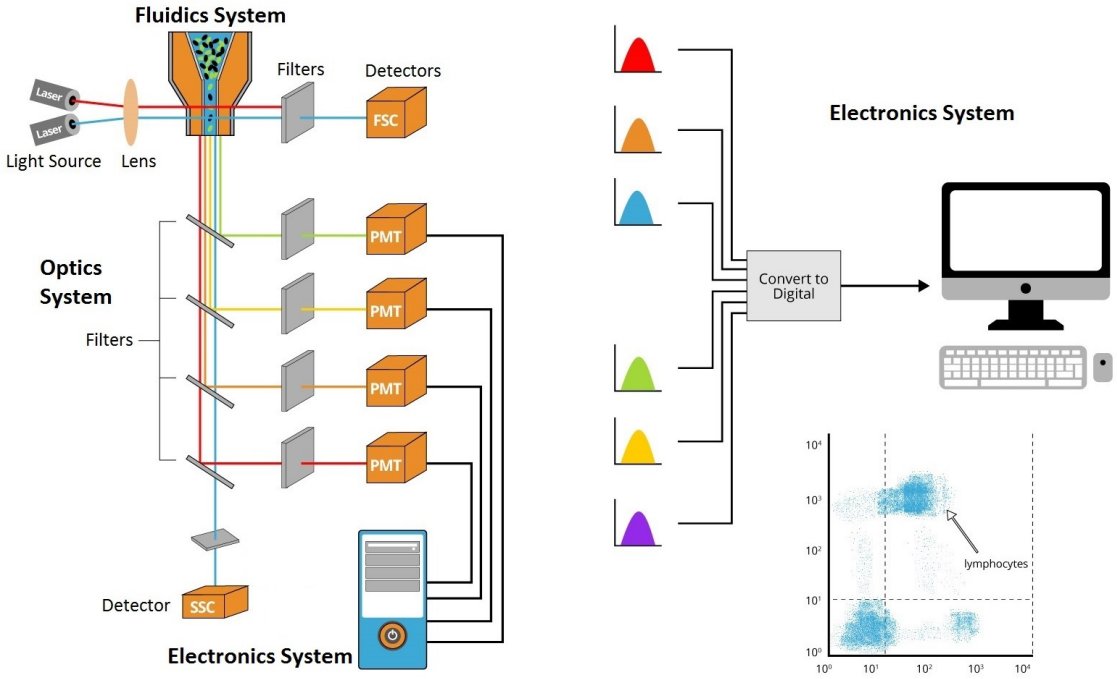

Figure 7: Schematic overview of a typical flow cytometry setup (https://www.bosterbio.com/protocol-and-troubleshooting/flow-cytometry-principle).

2.3.2. Flow cytometry applications

Flow cytometry has a wide spectrum of applications. One of the newest applications is in the field of infection biology, where flow cytometry is used for cell counting, internalization score, and subcellular patterns of co-localization for intracellular pathogen *Toxoplasma gondii* (Haridas et al., 2017).

Also, flow cytometry was used for phenotypic readout of the digestive vacuoles of *Plasmodium falciparum* which were treated with drugs and screened to identify drugs that are able to disrupt the digestive vacuole of the parasite (Chia et al., 2017). There are even methods of identifying and quantifying each of the four parasite blood stages of *Plasmodium falciparum* (Dekel et al., 2017). Imaging flow cytometry was used to survey the morphological features of *Blastocystis* subtypes species complex composed of 19 subtypes (Yason and Tan, 2015).

Flow cytometry is also used in the clinical laboratories for a variety of analyses including diagnostic immunophenotyping, DNA content analysis for prognosis of malignancies, screening of hematologic disorders, analyses of lymphocyte profiles, evaluation of peripheral stem cell products for transplantation, monitoring monoclonal antibody therapy and so on (Akao et al., 2018; Bakke, 2001; Betters, 2015). This technique can be even applied to the analysis of plankton samples. Flow cytometry can be used to measure phytoplankton composition on the basis of biovolume and chlorophyll (Becker et al., 2002; Brown and Wittwer, 2000; Olson et al., 1983; Trask et al., 1982).

2.3.3. DNA content and ploidy analysis

Flow cytometry has been widely used in the determination of ploidy level and DNA content (Yan et al., 2016). The measurement of cellular DNA content by flow cytometry uses fluorescent dyes, the most commonly used ones being DAPI, propidium iodide (PI), and 7-aminoactinomycin D (7-AAD). All these dyes intercalate into the DNA helical structure. The fluorescent signal is directly proportional to the amount of DNA in the nucleus (Brown and Wittwer, 2000; Darzynkiewicz et al., 2017).

Cellular ploidy is the number of complete sets of chromosomes in a cell. Many eukaryotic species have two (diploid) or one (haploid) sets of chromosomes. Sometimes, more than two (polyploid) sets of chromosomes can be identified which can be an effect of ancient whole genome duplication or hybridization events which happened during the evolution of plants, animals, and fungi. Ploidy changes also can occur at different stages of development of an organism and can vary within different tissues of the same organism and between individuals of the same species. Ploidy changes also arise during the sexual cycle of eukaryotes, from haploid gametes to diploid somatic cells. Aneuploidy represents an abnormal chromosome number and it is observed in novel environments, during periods of cellular stress, and during ploidy level changes. Ploidy is commonly measured by flow

cytometry of fluorescently labeled cells where the relative fluorescence of an unknown isolate is compared to strains with known ploidy (Poulíčková et al., 2014; Todd, Forche, & Selmecki, 2017).

Few studies for DNA content analyses were done for protists. For example a study on genus *Micrasterias* tried to analyze the interspecific and intraspecific DNA content variation by measuring the DNA content for 34 different strains to find out if the phylogeny of the genus *Micrasterias* is associated with DNA content variation in order to evaluate the evolutionary importance of polyploidy in the genus *Micrasterias* (Poulíčková et al., 2014). It was found a strong correlation between nuclear DNA content and chromosome number in the strains of genus *Micrasterias* and significant positive correlation between DNA content and cell size and morphology in the species *Micrasterias rotata.* Also, the authors showed the importance of life cycle studies for interpretation of DNA content measurements in microalgae (Poulíčková et al., 2014).

DNA content analysis by flow cytometry was successfully used for comparative analysis and ploidy investigation between *Trypanosoma cruzi* and *T. rangeli* isolated from different hosts, where propidium iodide (PI) staining was used, showing that DNA content analysis by flow cytometry can be successfully used for discrimination between this two species, when G1 peaks for strains of each species are distinct (Naves et al., 2017). Flow cytometry was also used for monitoring the changes in the DNA content and nuclear and cell morphology during cell cycle of *Alexandrium minutum* (Dapena et al., 2015).

Another interesting study focused on genome size analyses was done on chrysophytes where authors analysed the genome sizes beetwen heterotrophic, mixotrophic and phototrophic strains. The genome size was generally correlated with cell volume and it increased as the cell volume increased. The study suggested that the cell volume is the dominant factor in determining genome sizes, thus all factors that influence cell size should also affect genome size evolution (Olefeld et al., 2018). Another study focused on the genomes of nine species members of the Trichomonadea group. Here the genomes were estimated using flow cytometry using the genome of *Trichomonas vaginalis* as a calibration point (Zubáčová et al., 2008). The authors showed that the largest genomes were in the *Trichomonas* and *Tritrichomonas* genera (133–177 Mbp) and the smallest genome was the genome of *Tetratrichomonas gallinarum* (86 Mbp). As in the case of the other studies mentioned above, this study also showed that the genome size is correlated with the cell volume and size. (Zubáčová et al., 2008).

3. The aims of the work

- To analyse ploidies of various strains of *Monocercomonoides* using FISH against single copy genes.

- To analyse karyotypes of various strains of *Monocercomonoides* using FISH against telomeric repetitions.

- To estimate the genome sizes and DNA content of various strains of *Monocercomonoises* using flow cytometry.

4. Materials and methods

4.1. Cultivation of the investigated strains

All investigated strains are established cultures of oxymonads cultivated in our laboratory. Each of the cultures are regularly inoculated once a week into fresh TYSGM-9 medium (Diamond, 1982). All *Monocercomonoides* strains used in this study are growing in xenic cultures with an admixture of bacteria. The cultures are inoculated in bacterized TYSGM-9 media. The bacterization consists in inoculation of one drop of bacteria mixture into 10 ml media one-week prior inoculation of *Monocercomonoides*. The inoculated and bacterized cultures are kept at room temperature (most of the strains) or at 37^{o} C (in case of *Monocercomonoides exilis* strain PA203).

Most of the investigated strains were isolated from reptiles, two of them were isolated from cesspits and one single strain was obtained from a vertebrate host. The list of the studied strains and their original host is presented in Table 1.

Table 1: Studied strains of *Monocercomonoides*.

Species name	Strain	Host
Monocercomonoides exilis	PA203	*Chinchilla lanigera*
Monocercomonoides sp.	ERYM1	*Eryx* sp.
Monocercomonoides sp.	Mural1	*Podarcis muralis*
Monocercomonoides acer	TENE79	*Testudo marginata*
Monocercomonoides sp.	OEV	*Ophisops elegans*
Monocercomonoides sp.	LEI	*Leiocephalus carrinatus*
Monocercomonoides merkovicensis	Marek2	Cesspit
Monocercomonoides merkovicensis	VAV1B	Cesspit

4.2. Composotion and preparation of culture media

4.2.1. TYSGM – 9 (Diamond, 1982)

The components of the TYSGM-9 media are summarized in Table 2. All components except horse serum are dissolved in about 950 ml of distilled water and the pH is adjusted to 7,2. After adjusting the pH, we bring up the volume to 970 ml. The prepared media is

sterilized by autoclaving. After autoclaving 30 ml of inactivated horse serum is added. The media is aliquoted in 15 ml centrifuge tubes and stored in fridge at 4°C.

Table 2: The composition of TYSGM-9 media. The values represent the amount needed to prepare one liter of media.

Component	Amount
Tryptone	2 g
Yeast extract	1 g
K_2HPO_4	2.8 g
KH_2PO_4	0.4 g
NaCl	7.5 g
Distilled water	970 ml
Inactivated horse serum	30 ml

4.2.2. SOC media

SOC (Super Optimal broth with Catabolite repression) medium is used for the recovery of transformed bacterial cells. SOC maximizes the transformation efficiency of competent cells. The components of the media are presented in Table 3. The media without glucose is prepared and sterilized by autoclaving. Afterwards the glucose is added under sterile conditions to the autoclaved media. The prepared media is then aliquoted in 1.5 ml microcentrifuge tubes and stored at -20 °C.

Table 3: The composition of SOC media. The values represent the amount needed to prepare one liter of media.

Component	Amount
Tryptone	20 g
Yeast extract	5 g
10 mM NaCl	0,584 g
2.5 mM KCl	0,186 g
$MgCl_2$ (Anhydrous)	0,952 g
1M sterile glucose solution	20 ml

4.2.3. Liquid LB medium (Bertani, 1951)

LB media (lysogeny broth) is used as a growth medium for the transformed bacteria. The media is provided in powdered form and it is dissolved in water (Table 4). After dissolving the media is sterilized by autoclaving.

Table 4: Composition of liquid LB Broth medium. The values represent the amount needed to prepare 500 ml of media.

LB Broth (Sigma)	10g
Distilled water	Add to 500 ml

4.2.4. Solid LB medium (Bertani, 1951)

The solid LB media is a mixture of LB broth and agar which is then poured into Petri dishes and it was used for plating of the transformed bacteria. The components of the media are presented in Table 5. The Powder LB broth was dissolved in distilled water and bacteriological agar was added to the media. The media was sterilized by autoclaving and after mild cooling it was poured into Petri dishes under sterile conditions.

Table 5: Mixture of LB Broth and agar at Petri dishes. The values represent the amount needed to prepare a 500 ml of media.

LB Broth (Sigma)	10 g
Agar (Oxoid)	6 g
Distilled water	Add to 500 ml

4.3. Culture filtration

To minimize bacterial contamination before the isolation of DNA it was necessary to filter the culture of *Monocercomonoides* sp. The filtration procedure was similar to the one described by Hampl (Hampl et al., 2005). First, the culture was filtered through a filter paper to remove big aggregates of bacteria. Then the flow through was filtered through a 3.0 µm polycarbone filter membrane (Whatman). To speed up the filtration, partial pressure was applied by pipetting. At this stage the bacteria can pass through the filter, but most *Monocercomonoides* cells are retained. After initial filtration, the cells were washed two times using TYSGM-9 media without added horse serum. After filtration, the concentrated cells

were collected in 50 ml centrifuge tubes. It is important to filter the culture as fast as possible because the cells are sensitive to oxygen.

4.4. DNA isolation

The cells collected after filtration were centrifuged for 10 minutes at 1200 g at 4°C. The supernatant was discarded and pellet was resuspended in 200 µl of sterile PBS. The DNA was isolated using DNeasy® Blood & Tissue Kit (Qiagen) according to the manufacturer's protocol, and the DNA was eluted twice in 50 µl of elution buffer. The quantity and the quality of the DNA was estimated using a spectrophotometer (NanoDrop 2000 UV-Vis spectrophotometer, Thermo Fisher Scientific).

4.5. Isolation and fixation cells for FISH

Initially the culures of different strains of *Monocercomonoides* sp. were filtered using the procedure described above. The filtered cells were centrifuged for 10 minutes at 1200 g at 4°C. The supernatant was removed and the cells were hypothonised with 75mM KCl for 5 minutes at RT followed by centrifugation for 10 minutes at 1200 g at 4°C. After centrifugation the hypotonic solution was removed and the cells were fixed in 15 ml of methanol acetic acid 3:1 mixture for 20 minutes at RT. The fixed cells were harvested by centrifugation and resuspended in 500 µl methanol acetic acid 3:1 and stored at 4ºC.

4.6. Isolation and fixation cells for flow cytometry

Similarly to the cells used in FISH, the cells used for flow cytometry were also filtered using the method described above. The filtered cells were divided into three 15 ml tubes each of them containing 14 ml of culture. The cells were then fixed by adding formaldehyde into each tube to a final concentration of 1 % and incubated for 20 minutes on ice followed by centrifugation for 10 minutes at 1200 g at 4°C. After centrifugation the supernatant was discarded, and the cells were washed three times in 5 ml of PBS and pelleted by centrifugation at same conditions as described above. Finally, the pellet was resuspended in 1ml LB-01 solution (Dolezel et. al., 1989) and the suspension was passed through a 20 µm Nylon Net membrane (Milipore). Then the cells were strained using DAPI at a final concentration of 1µg/ml and used immediately for flow cytometry measurement.

4.7. Amplification and electroforesis

For amplification of the SufDSU gene from our *Monocercomonoides* strains we designed specific primers based on the alignment of the SufDSU genes from *Monocercomonoides exilis, Blattamonas nauphoetae* and *Paratrimastix pyriformis.* The designed primers are shown in the Table 6. Amplifications were carried out using PrimeSTAR® Max DNA Polymerase Premix. The reaction mixture was prepared according to the manufacturer's recomandation and it is detailed in Table 7 and the PCR conditions for amplification are presented in Table 8.

Table 6: Designed primers for SUFDSU.

Title of sequence	Sequence 5′ → 3′
SU-OX-F1	SYCKSTSRTYTACCTCGACAACG
SU-OX-F2	CATYRTKCTSACTGAGCTGGAGCA
SU-OX-R1	GAYGCRCACTTCACWCGCGACGGG
SU-OX-R2	GTYGTGATGAGSYSGTGGAACTGC

Table 7*:* The reaction mixture with PrimeSTAR® Max DNA Polymerase Premix.

Components	Volume
2 x Premix (Primer Star Max)	12,5 µl
Primer F (SU-OX-F1, SU-OX-F2)	1,25 µl
Primer R (SU-OX-R1, SU-OX-R2)	1,25 µl
DNA	1 µl
H_20	Add to 25 µl

Table 8: Cycler parameters used with PrimeSTAR® Max DNA Polymerase.

Part of the cycle	Number of cycles	Temperature	Time
Initial denaturation	1 x	98°C	4 min
Denaturation	36 x	98°C	0:10 min
Annealing		61°C	0:15 min
Elongation		72°C	0:15 min
Final elongation	1 x	72°C	5 min

The preparation of the DNA template for telomere repeats was done according to the protocol described in Ijdo et al 1991 (Ijdo et al., 1991) with following modifications: the extension time was halved and *Taq* polymerase was replaced with Q5 polymerase to minimize polymerase errors during the synthesis. The reaction mixture was done according to the Table 9. The PCR was carried out in the absence of template using primers $(TTAGGG)_5$ (Telo F) and $(CCCTAA)_5$ (Telo R). Amplification consisted of 15 cycles with 1 minute at 94°C, 30s at 55°C and 30s at 72°C, followed by 40 cycles with 1 minute at 94°C, 30s at 60°C, 45s at 72°C and finally 5 minutes at 72°C. The cycler parameters are summarized in the Table 10.

Table 9: The reaction mixture for amplification of telomeric repeats using Q5 polymerase.

Components	Volume
5 x Q5 reaction buffer	10 µl
10mM dNTPs	4 µl
10µM Telo R	0,5 µl
10µM TeloF	0,5 µl
Q5 polymerase	0,5 µl
Nuclease-free H_2O	Add to 50 µl

Table 10: Cycler parameters used with Q5 polymerase for amplification of telomere repeats.

Part of cycle	Number of cycles	Temperature	Time
Denaturation	14 x	94°C	1 min
Annealing		55°C	0:30 min
Elongation		72°C	0:30 min
Denaturation	40 x	94°C	1 min
Annealing		60°C	0:30 min
Elongation		72°C	0:45 min
Final elongation	1 x	72°C	1 min

To check for the presence of the desired amplified PCR products we performed horizontal electrophoresis. For this we a prepared 1% agarose gel in an Erlenmayer flask

consisting of 0,4 g of agar (Gibco) and 40ml TAE buffer (1x). The mixture was boiled to dissolve the agar, then the solution was slightly cooled down and 40µl of SYBR safe (LifeTechnologies) was added. The gel was poured into a casting tray and a comb was added then the gel was left to solidify for about 20 minutes. After solidification we placed the gel into an electrophoresis tank and added TAE buffer to completely cover the gel with buffer. Afterwards, we loaded our samples together with a DNA ladder. Usually we loaded 5 µl of our sample which was mixed with 1 µl of loading dye. The electrophoresis ran for about 30 minutes at 100V, followed by examination of the gel under a transilluminator.

4.8. Gel extration and DNA purification

In situations where only one band was present after the PCR amplification the sample was purified directly using High Pure PCR Product Purification Kit (Roche) according to the manufacturer's protocol. When multiple bands were present in our PCR reaction, the correct band was cut out from the gel using a sterile scalpel and placed in a sterile microcentrifuge tube. Then the DNA was extracted using QIAquick Gel Extraction Kit (Qiagen) according to the manufacturer's protocol. The eluted DNA was measured using nanodrop. The purified DNA was used for sequencing and later for cloning.

4.9. Clonning

For probe labeling and sequencing the purified products were initially cloned into pJet vector using CloneJet PCR Cloning kit (Thermo Scientific) and TOP10 competent cells.

Table 11: The reaction mixture for the ligation.

Component	Volume
2x reaction buffer	10 µl
Purified PCR product	use in a 3:1 molar ratio with pJET 1.2/blunt (in case of 2200kb fragment we used 100ng of DNA; for 1700kb fragment 85ng DNA)
pJET1.2/blunt cloning vector (50ng/µl)	1 µl
Water, nuclease free	Up to 19 µl
T4 DNA ligase	1 µl

The CloneJet PCR Cloning kit contains a zero-background vector, which means that the bacteria which do not contain any insert in the vector will not grow on the plate. The ligation reaction mixture is summarized in Table 11.

The ligation mixture was vortexed briefly and centrifuged for few seconds followed by incubation at RT for 30 minutes. After incubation, the ligation mixture was pipetted on competent cells and the cells were incubated 30 minutes on ice, followed by a heat shock for 45 seconds at 42°C. After heat shock the cells were placed immediately on ice for 2 minutes. Then 250µl of SOC media was added and the bacteria were incubated for recovery for 60-90 minutes by shaking at 37°C. Meanwhile we prepared LB plates with ampicillin by adding 30 µl of ampicillin on the plate (stock solution 100mg/ml, Sigma) and plating it. After incubation 150 µl of bacteria were plated on LB plates and incubated overnight at 37°C.

Next day 10 bacterial colonies were randomly selected and we did colony PCR using *EmeraldAmp® MAX PCR Master Mix.* We prepared the mixture for colony PCR (Table 12) and finally a small part of the colony was directly added in the tube using a pipette tip. Then we run the colony PCR using the parameters described in Table 13.

Following colony PCR we did horizontal electrophoresis to check if we colony contains the right insert and decided which colonies will be used for further analysis and plasmid isolation. For plasmid isolation the selected colonies were cultured in 15 ml centrifuge tubes with 4 ml LB media + 4 µl AMP (stock solution 100mg/ml). The colony was inoculated directly into the tube using a pipette tip and the tubes were incubated overnight at 37°C with agitation

Table 12: Reaction mixture with EmeraldAmp® MAX PCR Master Mix.

Components	Volume
Master mix	12,5 µl
Primers F used	1,25 µl
Primers R used	1, 25 µl
H_2O	10 µl

Table 13: Cycler parameters used with with EmeraldAmp® MAX PCR Master Mix for colony PCR

Part of the cycle	Number of cycles	Temperature	Time
Initial denaturation	1 x	95°C	5 min
Denaturation	35 x	95°C	0:30 min
Annealing		55°C	0:30 min
Elongation		72°C	2:30 min
Final elongation	1 x	72°C	7 min

.

Next day, the culture was centrifuged at 6000g at 5 minutes. The supernatant was discarded and we isolated the plasmid from the pellet using High Pure Plasmid Isolation kit (Roche). Then we measured the concentration of the DNA by spectrophotometer (NanoDrop 2000 UV-Vis spectrophotometer, Thermo Fisher Scientific). The resulting DNA was used for sequencing.

4.10. Sequencing

Sequencing reactions were prepared by mixing H_2O, primer and DNA into a microcentrifuge tube to a final volume of 8 µl (Table 14). For sequencing of the fragments from plasmids we used PJF and PJR primers, which are complementary to plasmid, but we also used our specific primers (Table 6). The sequencing was done by the OMICS core facility in BIOCEV.

Table 14: Sequencing reaction components.

Component	Amount
H_2O	Add to 8 µl
Primer	0,5 µl
DNA	2-5 ng DNA/100bp

4.11. Sequence assembly and phylogenetic analysis

The DNA chromatographs which we received from the sequencing facility were analyzed and assembled using Geneious program. After assembly the primer sequences were removed and resulting contig was saved as a FASTA file, and added to our dataset. For phylogenetic analysis of the SufDSU gene we used a dataset containing known oxymonad sequences and another eukaryote or bacterial sequences including sequences from various unpublished oxymonad genomes on which we are working in our laboratory. This dataset was kindly provided by Vojtěch Vacek and consisted of 162 sequences plus five new sequences which we amplified. The alignment of the sequences was made on the MAFFT server (Katoh and Standley, 2013) using default parameters. Alignment was automatically trimmed using BMGE (Criscuolo and Gribaldo, 2010) with the matrix BLOSUM 30. The final alignment contained 281 amino acid positions. A maximum likelihood phylogenetic tree was constructed using using RAxML version 8.2.7 (Stamatakis, 2006) with the LG model. Branch support was estimated by bootstrapping with 1000 replicates. The resulting phylogenetic tree was viewed in FigTree, v1.4.3 (http://tree.bio.ed.ac.uk/software/figtree/), and adjusted using Inkscape.

4.12. Probe Labelling

For labelling we re-amplified the SufDSU genes from our isolated plastids which contained the cloned sequence. For this, we diluted the plastid 1:100 with water and used 1 µl of the diluted plastid as a template for PCR amplification using PrimeSTAR® Max DNA Polymerase Premix. PCR conditions for amplification are presented in the Table 8. After amplification, the fragment was checked by gel electrophoresis, followed by purification using High Pure PCR Product Purification Kit (Roche). The labeling mixture is summarized at the Table 15. For labeling we used DecaLabel DNA Labeling Kit (Thermo Fisher Scientific). First, we mixed 1 ug of DNA + 10µl of decanucleotide in 5x reaction buffer and water was added to 42µl. The mixture was vortexed and centrifuged briefly. This mixture was denatured by boiling for 10 minutes, then placed immediately on ice for 3 minutes. To the denatured mixture, we added 5µl of dNTP mix, 1,75µl Digoxygenin-11-dUTP (Roche) and water to final volume 50µl. The mixture was incubated overnight at 30°C. The next day we purified the labeled probe using QIAquick Gel Extraction Kit (Qiagen) and eluted it in a final volume of 50µl.

Table 15: Components of the labelling mixture.

Component	Volume
Decanucleotide in 5 x reaction buffer	10 µl
DNA	1 µg
H_2O	Add to 42 µl
Non-radioactive labelling mix (dNTP mix)	5 µl
1mM Digoxygenin-11-dUTP (Roche)	1,75 µl
Klenow fragment	1 µl
H_2O	Add to 50 µl

4.13. Fluorescence *in situ* hybridization

For FISH analysis we used the protocol described by Zuzana Zubáčová (Zubáčová et al., 2011) which was slightly modified for our experiments. For FISH preparations we used Superfrost slides (Thermo Fisher Scientific).

First, the hypotonized and fixed cells were dropped on the slide from a height of about 30 cm and left to air dry at room temperature. Then the slides were immersed for a second in 50% acetic acid, to remove the cytoplasmic residues, and dried at 37°C, followed by incubation in 50 µg/ml pepsin (Sigma) in 3mM potassium acetate and 0,01M HCl for 5 minutes at 37°C. Then the slides were washed in phosphate-buffered saline (PBS) pH 7.4 at RT for 5 minutes. Subsequently the samples was post fixed with 2% formaldehyde in PBS for 30 minutes at RT.

Afterwards, the slides were washed tree times in PBS at RT. To remove any endogenous peroxidases and minimize background, the slides were incubated in 3% H_2O_2 for an hour at RT followed by dehydration in series of 70% 90% and 100% methanol for 3 minutes in each. Afterwards 50 µl of hybridization mixture containing the probe in 50% deionized formamide and 2 x SSC was added on the slides. The amount of the probe for telomeric repeats was always 0,1 µl, but for SufDSU the amount of the probe was 0,2 µl in case of *Monocercomonoides* sp. strain LEI and for *Monocercomonoides* sp. strains Mural1 and OEV, and *Monocercomonoides merkovicensis* strains Marek2 and VAV1B we used 0,5 µl of the probe. After adding the hybridization mixture on the slide, the slide was covered

with a coverslip and denatured at 82°C for 5 minutes. After denaturation the edge of the slide was sealed with rubber cement and incubated over night at 37°C in a wet chamber.

Next day, the coverslips were removed and the slides were washed three times for 5 minutes at 45°C in 50% formamide (Fluka) in 2 x SSC, followed by three washes for 5 minutes in 2 x SSC at 45°C. After stringency washes the slides were washed once more in TNT buffer (100 mM Tris–HCl, 150 mM NaCl, 0.05% Tween 20, pH 7.5) at RT by shaking for 5 minutes. Then the slides were blocked in TNB blocking buffer (PerkinElmer) for 30 minutes in a wet chamber, followed by incubation with antibody for one hour. For single copy gene FISH were used anti-digoxigenin antibody conjugated with horseradish peroxidase (Roche) diluted 1:2000 in TNB buffer. For telomeric FISH we used anti-digoxigenin antibody conjugated with Dylight 488 diluted 1:2000 in TNB buffer. After incubation with the antibody the slides were washed three times for 5 minutes in TNT buffer by shaking at RT. For preparations which were used for telomeric FISH after washing in TNT buffer we finally washed the slides for three minutes in MilliQ water and air dried. For single copy gene FISH preparations we did tyramide signal amplification (TSA) using the TSA – Plus TMR System (PerkinElmer), according to the manufacturer's protocol. For amplification the slides were incubated for 5 minutes with the amplification mixture containing 2 µl of fluorophore plus 98 µl amplification diluent plus 0,33 µl of 0,1 % H_2O_2. The amplification time was adjusted in such a way to minimize background, in our case 5 minutes of amplification was estimated to be optimal. Afterwards, the slides were washed three times for 5 minutes in TNT buffer and one time for three minutes in MilliQ water and air dried.

Finally, the slides were mounted using Vectashield mounting medium with DAPI (VectorLabs). The slides were analyzed using IX81 Olympus microscope equipped with an IX2-UCB camera. The acquired images were deconvolved using Huygens 16.10 and further processing was done using ImageJ.

4.14. Flow cytometry

We tried to estimate DNA content of various *Monocercomonoides* strains using flow cytometry. For this we measured the fluorescence of DAPI stained cells from various strains of *Monocercomonoides* and compared it to *Monocercomonoides exilis* strain PA203 which was used as a reference, knowing that its haploid genome size it is approximately 82 Mbp (Hampl, personal information).

For flow cytometry the cells were fixed as described in the chapter 6.5. Prior measurement the samples were kept on ice. Stained nuclei were analyzed with BD LSRFortessa^{TM} flow cytometer. At least 10000 cells were measured for each sample.

DNA content was estimated according to Dolezel (Dolezel et al., 1992). The emitted fluorescence is proportional to DNA content, and the fluorescence ratio (FR) is equal to the ratio of the genome sizes FR = GSs / GSr, where GSr is the genome size of the reference and GSs is the genome size of our strain. Thus, the genome size of a sample can be calculated as GSs = GSr x FR. Conversion between the DNA content and genome size was made using the conversion factor 1 pg of DNA = 978 million base-pairs (Mbp) (Dolezel et al., 2003).

5. Results

5.1. Ploidy analyses

5.1.1. Amplification of single copy genes and phylogenetic analysis

To analyse the ploidy of our selected *Monocercomonoides* strains we used FISH against single copy genes. We decided for SufDSU gene which is known from genome sequence of *M. exilis* to be a single copy gene. Our primers were designed in such a way to amplify the fusion of the SufS and SufU parts of the SufDSU. The primers were designed based on the alignment of the SufDSU genes from *Monocercomonoides exilis, Blattamonas nauphoetae* and *Paratrimastix pyriformis* and are shown in Table 6. For *Monocercomonoides mercovicenis* strains Marek2 and VAV1B and *Monocercomonoides* sp. strain OEV we used primers SU-OX-F1 and SU-OX-R1, which amplified fragment about 2000bp. For *Monocercomonoides* sp. strains LEI and Mural1 we used SU-OX-F2 and SU-OX-R2, which amplified fragment about 1700bp. For *Monocercomonoides* acer strain TENE79 and *Monocercomonoides* sp. strain ERYM1 we were not able to amplify the fragment of interest using our primers. The amplified fragment were subcloned in pJet Vector using TOP10 competent cells and completely sequenced. We did phylogenetic analyses to be sure that our obtained fragments are from oxymonads and group with other Preaxostyla on the tree. For this we used a dataset of 162 SufS sequences downloaded from NCBI which was provided by Vojtěch Vacek (Vacek et al., 2018) to which we added our sequenes. We aligned the sequences using MAFFT followed by manual examination and trimmed the alignment using BMGE with the matrix BLOSUM 30. The final alignment contained 281 amino acid positions. Phylogenetic tree from these sequences (Figure 8) was constructed by maximum likelihood method in program RAxML using LG model. Branch support was estimated by bootstrapping with 1000 replicates. Our phylogenetic analysis failed to clearly pinpoint the bacterial donor of the Suf system in oxymonads but clearly showed that our obtained sequences are of eukaryotic origin and group together with another oxymonad sequences.

Figure 8: Maximum likelihood (ML) tree of SufS gene. Values at the nodes represent the ML bootstrap support. Values below 50 are not shown besides the Preaxostyla branch. Sequences from Preaxostyla are highlighted in red, and sequences from photosynthetic organisms are highlighted in green. The branch length of *Legionella pneumophila* was shortered by 50%.

5.1.2. Single copy genes analyses

The subcloned SufDSU fragments were labelled with digoxigenin. The FISH protocol was performed according to the protocol described in Zubáčová et al. (Zubáčová et al., 2011) with some modifications as described in the chapter 4.13. The concentration of H_2O_2 was increased from 1% to 3% to reduce the background signal and also the probe concentration was reduced from 2 µl to 0,2 µl in the case of *Monocercomonoides* sp. strain LEI and 0,1 µl in the case of *Monocercomonoides* sp. strains Mural1 and OEV and *Monocercomonoides mercovicenis* strains VAV1B and Marek2 to reduce the background.

Table 16: Number of signals for for SufDSU gene in the 50 nuclei of *Monocercomonoides* strain.

Species	Strain	Number of nuclei with a single signal	Number of nuclei with double signals
Monocercomonoides sp.	OEV	49	1
	LEI	48	2
	Mural1	48	2
Monocercomonoides merkovicensis	Marek2	47	3
Monocercomonoides merkovicensis	VAV1B	50	0

For most of our strains the probe efficiency for the single copy gene was rather low. In most of the cases approximately 3 out of 10 nuclei had positive signal which means that the probe efficiency was around 30%. We analysed 50 nuclei containing at least one signal for each strain and counted the recorded the number of signals (Table 16). The FISH results suggest that all the strains are haploid, with most of the analyzed cells having one clear signal in the nucleus. Examples of nuclei are given in the Figure 9. In case of *Monocercomonoides* sp. strain OEV the cell nuclei had a lower DAPI intensity.

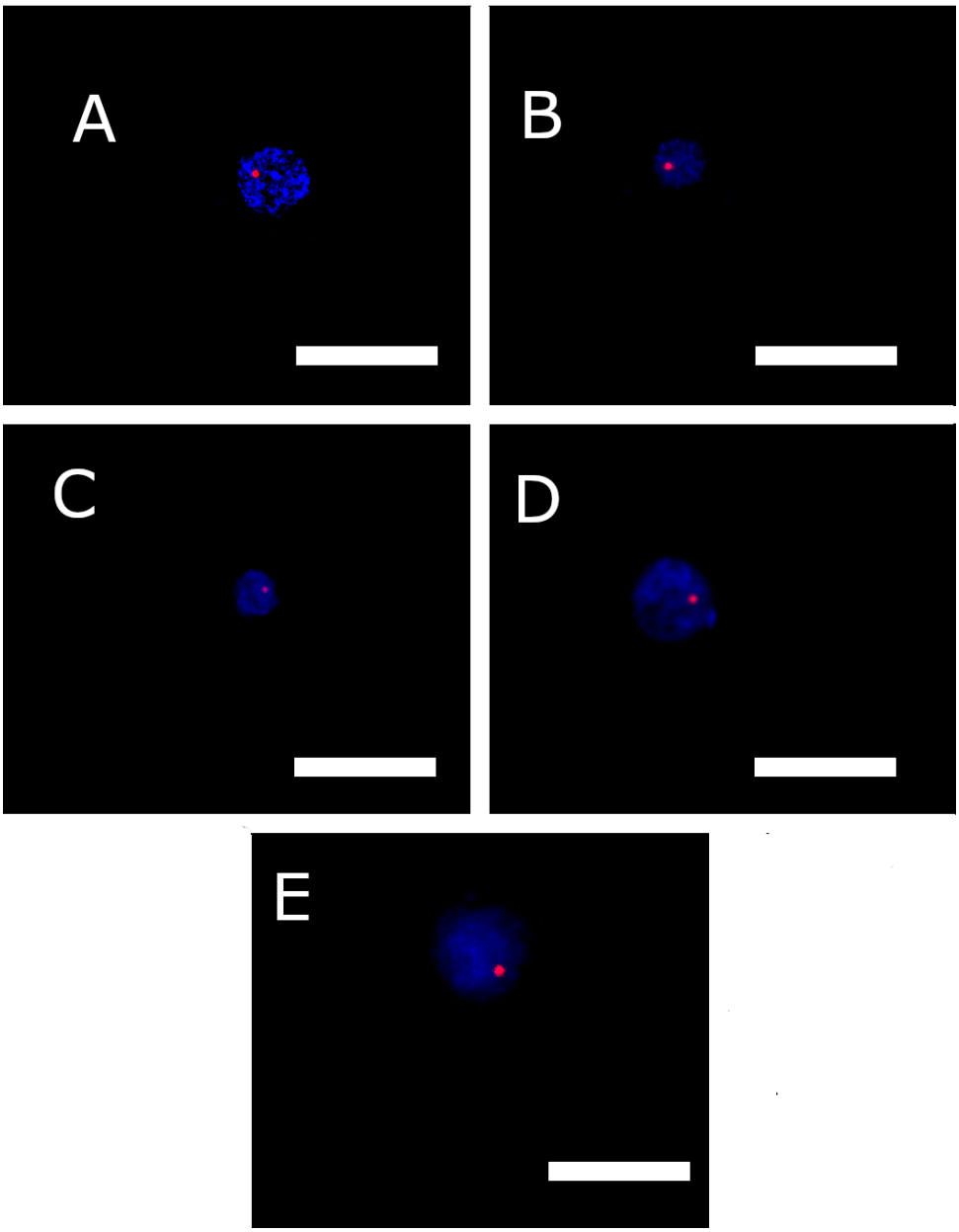

Figure 9: Fluorescence *in situ* hybridization using single copy genes suggest that all investigated strains are haploid. (A) *Monocercomonoides* sp. strain OEV, (B) LEI, (C) Mural1, (D) *Monocercomonoides mercovicenis* strain Marek2 and (E) strain VAV1B. Scale bar in all images indicates 5 µm.

5.2. Karyotype analyses

FISH was also used for the analysis of karyotype of our investigated strains. For this analysis we used protocol described by Ijdo et al (1991) to prepare the telomeric probes using primer dimer extension. In our case, the protocol was slightly modified by replacing Taq polymerase with Q5 polymerase and elongation times were halved. The PCR amplification was carried out using primers $(TTAGGG)_5$ (Telo F) and $(CCCTAA)_5$ (Telo R), and the obtained DNA was labeled with digoxigenin and detected by anti-digoxigenin antibodies conjugated with DyLight 488. Compared to the single copy genes, which were also labeled with digoxigenin, we did not use TSA system for signal amplification because the individual signals would be too strong, and we would not be able to distinguish between single signals from the nuclei and count them. The processing of the pictures and counting of telomeric signals was done using ImageJ program. 100 nuclei were analysed for each strain and the statistics is shown in the Figure 10. The average number of telomeric signals in the case of *Monocercomonoides* sp. strains LEI, Mural1, ERYM1, OEV and *Monocercomonoides acer* strain TENE79 were in between 9 and 17 (Figure 11), while significantly higher number of telomeric signals were observed in the nuclei of *M. mercovicensis* strains Marek2 and VAV1B (Figure 11), with an average number of signals of 58 and 107, respectively.

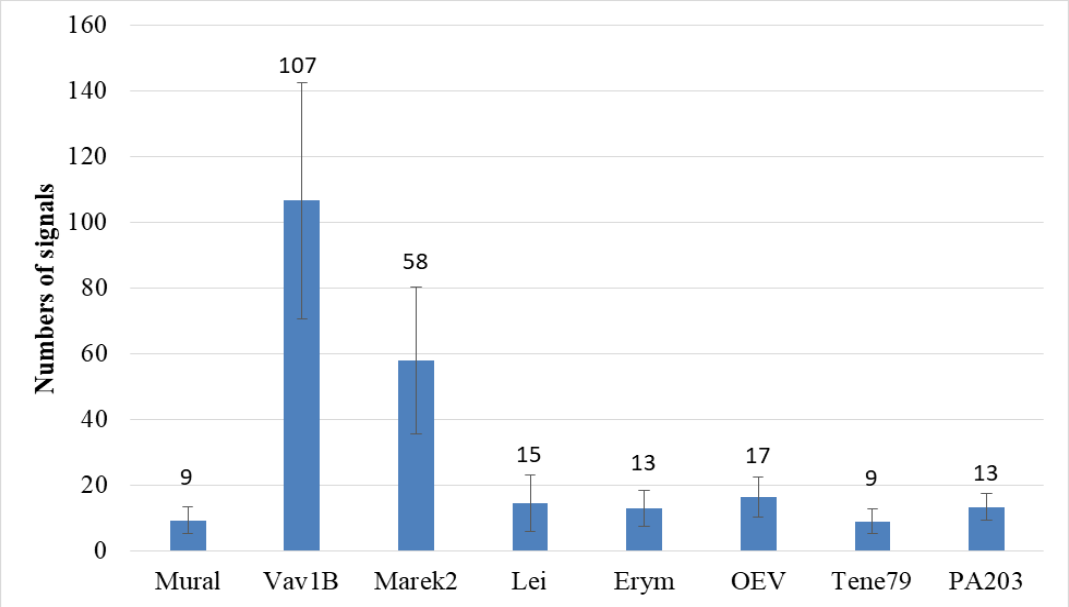

Figure 10: Number of telomeric signals for each investigated *Monocercomonoides* strain. The values on the graph represent the average number of signals, and the error bars represent the standard deviation.

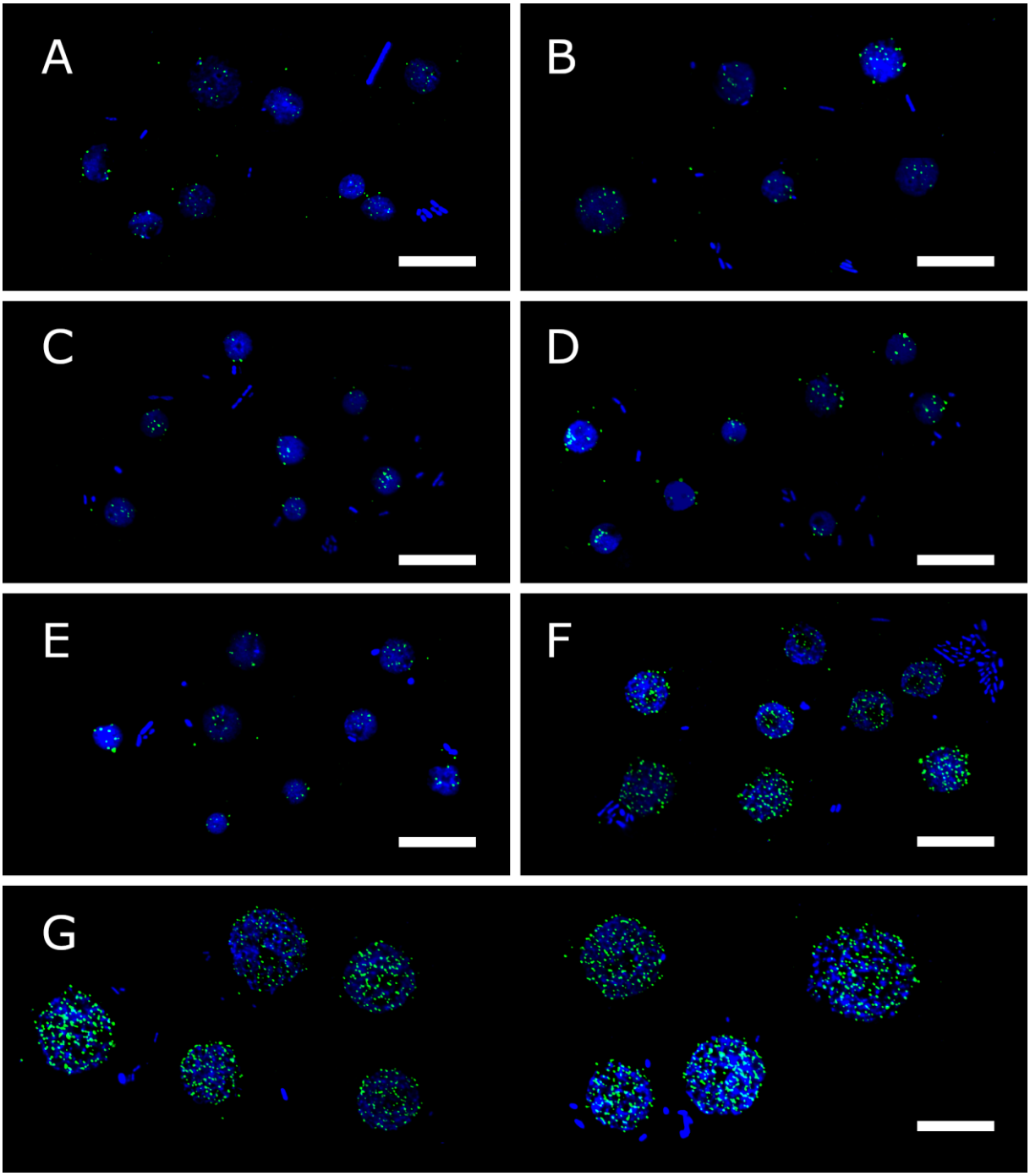

Figure 11: Fluorescence *in situ* hybridization using probes against telomeric repeats for investigated *Monocercomonoides* strains. (A) *Monocercomonoides* sp. strain OEV, (B) *Monocercomonoides* sp. strain LEI, (C) *Monocercomonoides* sp. strain ERYM1, (D) *Monocercomonoides acer* strain TENE79, (E) *Monocercomonoides* sp. strain Mural1, (F) *Monocercomonoides mercovicenis* strain Marek2 and (G) *Monocercomonoides mercovicenis* strain VAV1B. Scale bars indicates 10µm.

5.3. Genome size analyses

Flow cytometry was used for the analysis of DNA content of our investigated strains of *Monocercomonoides*. Cell were prepared as described in chapter 6.5, stained with DAPI and immediately measured using BD LSRFortessa flow cytometer. For the estimation of DNA content, we used the cells of *Monocercomonoides exilis* PA203 as standard, for which we know that the haploid genome size is approximately 82 Mbp. For *Monocercomonoides mercovicensis* strain VAV1B, *Monoccercomonoides* sp. strains OEV and Mural1 we succeeded to estimate the DNA content from three replicates, however, for *Monocercomonoides acer* strain TENE79 and *Monocercomonoides* sp. strain LEI we managed to measure it just two times and *Monocercomonoides* sp. strain ERYM1 was measured only once. We were not able to measure DNA content in *Monocercomonoides mercovicensis* strain Marek2, because it was not possible to distinguish between our investigated cells and bacterial aggregates or other debris, which were still retained in the sample even after filtration. The *Monocercomonoides exilis* used as standard was measured at the beginning of each session of the measurement to make sure that the calibration is accurate and there is not any variation which can be caused by the instrument. In the case of our PA203 standard, the histogram clearly shows a nice sharp peak for G1 and the G2 phase was also observed (Figure 12). For *Monocercomonoides* sp. strains OEV (Figure 13), Mural1 (Figure 14) and LEI (Figure 15) it seems that the DNA content is smaller compared to our reference with the estimated genome size being 30, 36 and 42 Mbp respectively (Figure 18). For *Monocercomonoides* sp. strain ERYM1 the DNA content was estimated to be around 69 Mbp (Figure 18) which is close to the DNA content of *Monocercomonoides exilis*, but here we managed to measure the cells just once and the histogram for this strain is not shown. *Monocercomonoides acer* strain TENE79 has an estimated DNA content of 106 Mbp (Figure 18) which is slightly bigger compared to *Monocercomonoides exilis* but from the histogram (Figure 16) we can see that the peak is really wide. *Monocercomonoides mercovicensis* strain VAV1B appears to have the biggest DNA content with the estimated size of about 129Mbp (Figure 18) but in this case the histogram is also really wide (Figure 17). The table with the summary values of DNA content for the investigated *Monocercomonoides* strains is shown in the Table 16.

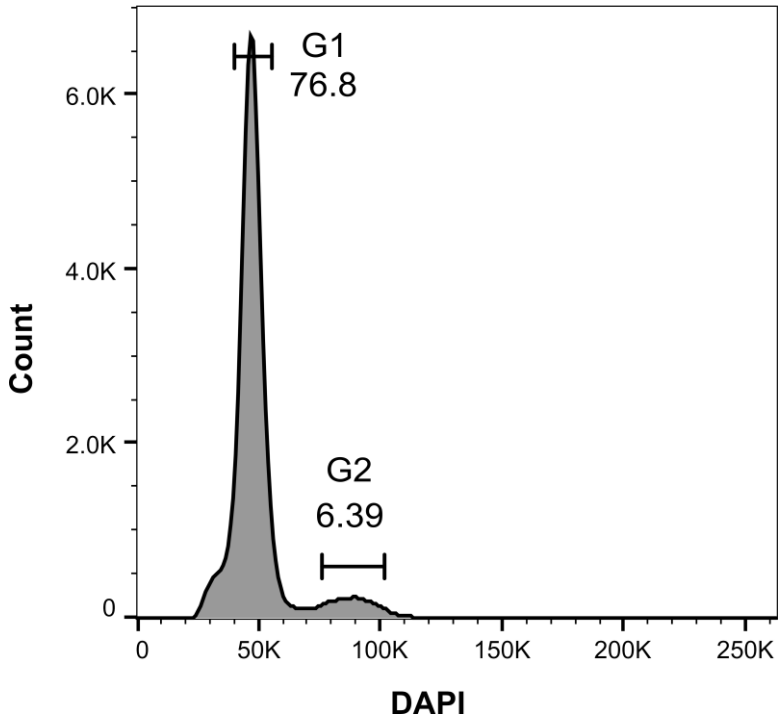

Figure 12: Histogram of fluorescence intensity corresponding to DAPI stained DNA in cells of *Monocercomonoides exilis* strain PA203. The Y-axis represents the number of cell counts and the X-axis is the relative fluorescence intensity of DAPI. G1 and G2 phases are clearly visible.

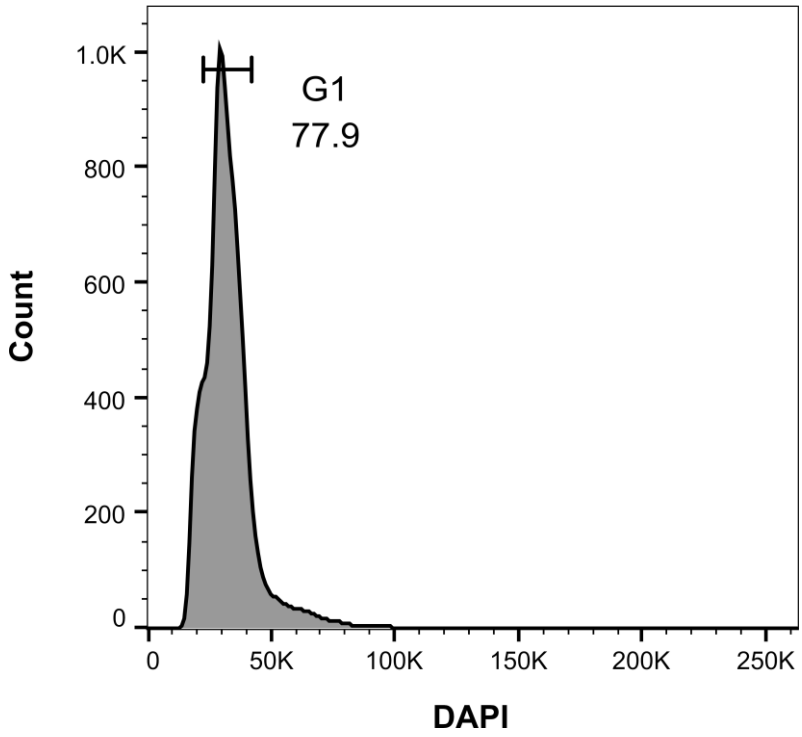

Figure 13: Histogram of fluorescence intensity corresponding to DAPI stained DNA in cells of *Monocercomonoides* sp. strain LEI. The Y-axis represents the number of cell counts and the X-axis is the relative fluorescence intensity of DAPI. G1 is clearly visible.

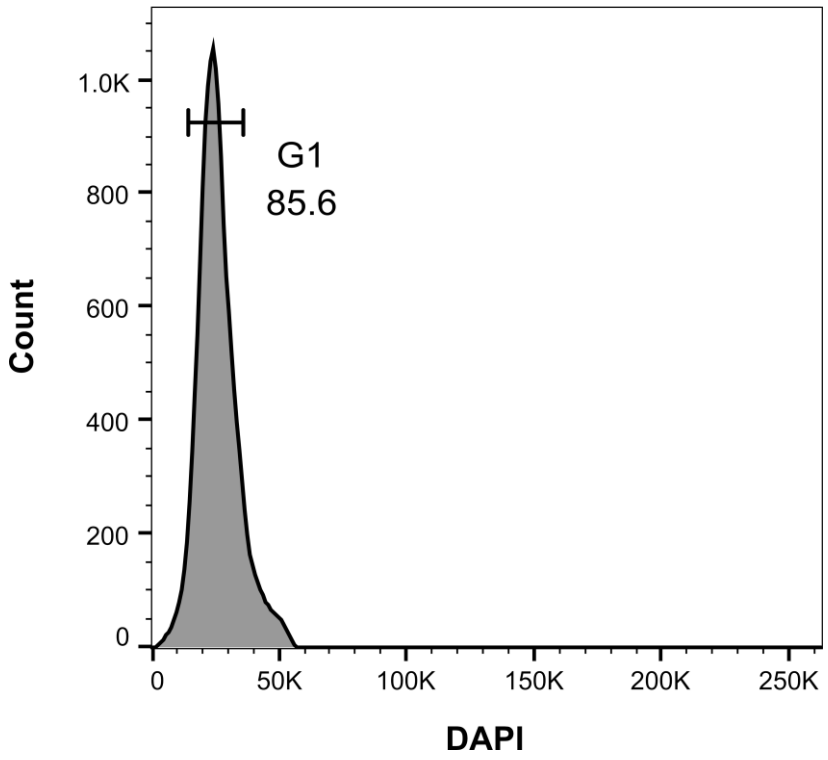

Figure 14: Histogram of fluorescence intensity corresponding to DAPI stained DNA in cells of *Monocercomonoides* sp. strain Mural1. The Y-axis represents the number of cell counts and the X-axis is the relative fluorescence intensity of DAPI. G1 is clearly visible.

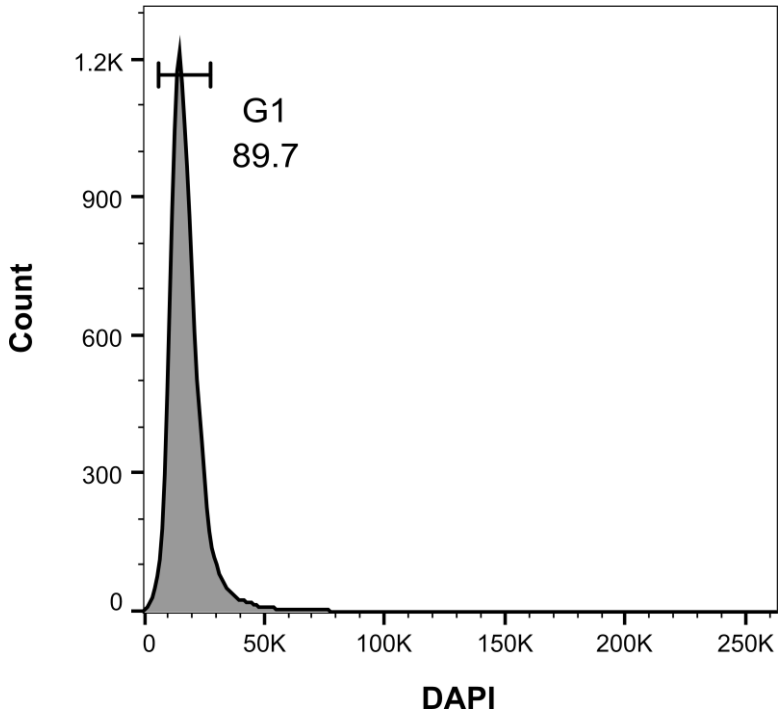

Figure 15: Histogram of fluorescence intensity corresponding to DAPI stained DNA in cells of *Monocercomonoides* sp. strain OEV. The Y-axis represents the number of cell counts and the X-axis is the relative fluorescence intensity of DAPI. G1 is clearly visible.

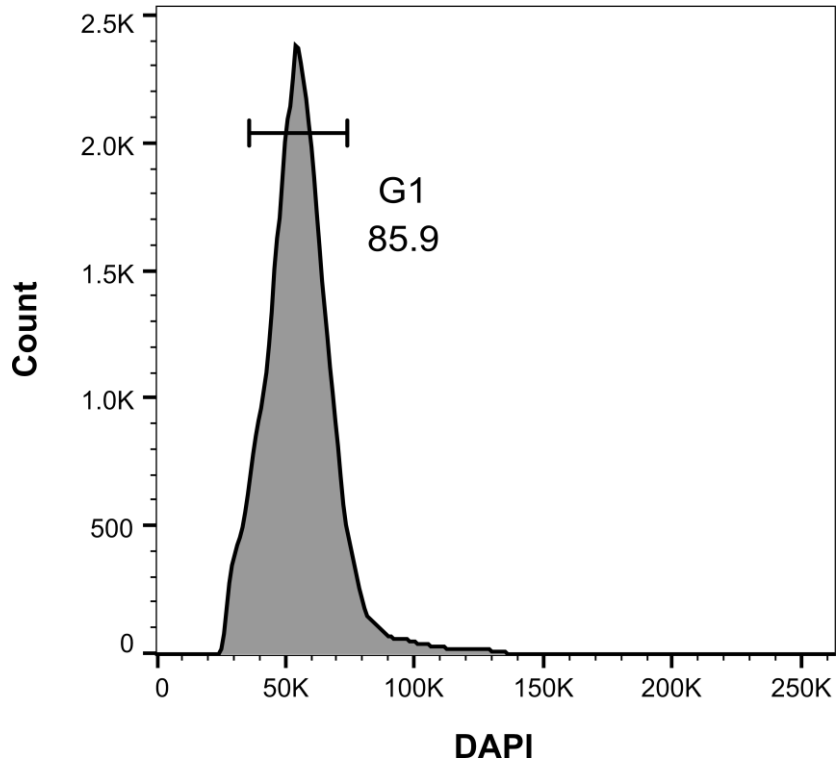

Figure 16: Histogram of fluorescence intensity corresponding to DAPI stained DNA in cells of *Monocercomonoides acer* strain TENE79. The Y-axis represents the number of cell counts and the X-axis is the relative fluorescence intensity of DAPI. G1 is clearly visible.

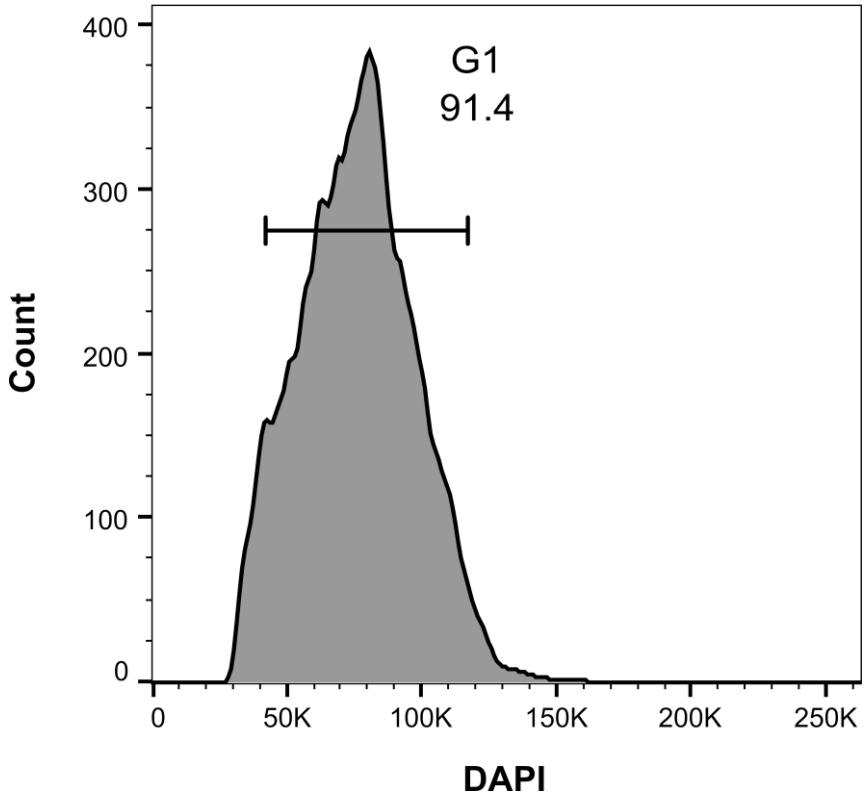

Figure 17: Histogram of fluorescence intensity corresponding to DAPI stained DNA in cells of *Monocercomonoides merovicenis* strain VAV1B. The Y-axis represents the number of cell counts and the X-axis is the relative fluorescence intensity of DAPI.

Table 16: DNA content estimation for investigated *Monocercomonoides* strains. The values represent average with standard deviation (for strains marked with * the measurement was not done in tree replicates).

Species	Strain	DNA content (Mbp)
Monocercomonoides sp.	OEV	30 ± 2.37
	Mural1	36 ± 5,05
	LEI*	42
Monocercomonoides acer	TENE79*	106
Monocercomonoides sp.	ERYM1*	69
Monocercomonoides mercovicenis	VAV1B	129 ± 2,79

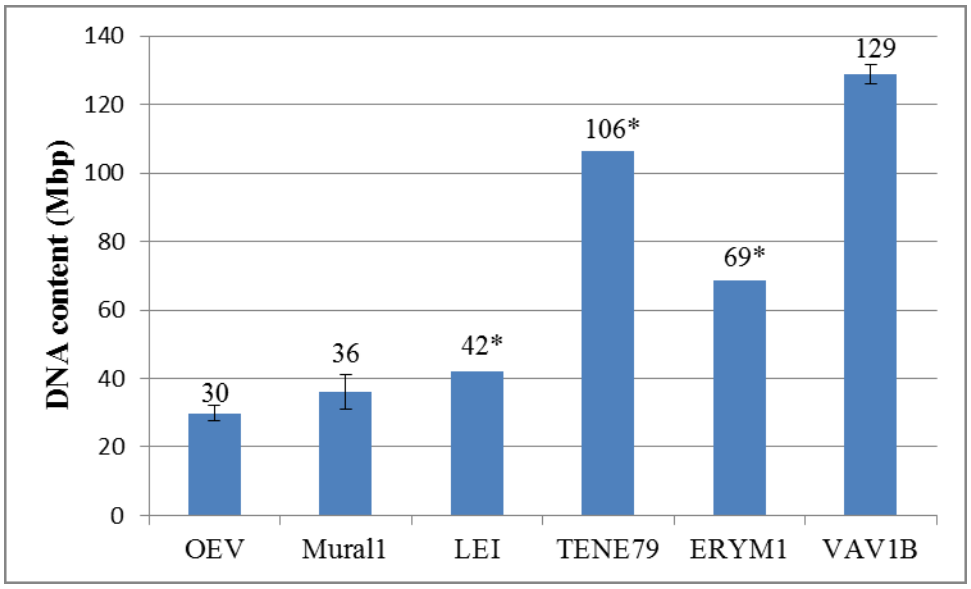

Figure 18: Estimated DNA content (Mbp) for the investigated *Monocercomonoides* strains. The values on the graph represent the estimated DNA content (Mbp) and the error bars represent the standard deviation. Strains marked with star were not measured three times.

6. Discussion

To analyze the ploidy of various species of *Monocercomonoides* we designed the primers for one single copy gene. We decided to use SufDSU gene which we know from genome sequences of *Monocercomonoides exilis* to be in a single copy. The primers were designed in the way to amplify the regions of SufS and SufU, which are specifically fused in oxymonads. We tried to amplify this part of gene for the seven strains of *Monocercomonoides* investigated, but we successfully amplified the sequences for *Monocercomonoides mercovicenis* strains VAV1B and Marek2 and *Monocercomonoides* sp. strains OEV, LEI and Mural1, but in the case of *Monocercomonoides acer* srain TENE79 and *Monocercomonoides* sp. strain ERYM1 we were not be able to amplify this fragment using any combination of our primers. This could be caused by the fact that *Monocercomonoides acer* strain TENE79 is more divergent in the sequence of this gene compared to the other strains. ERYM1 had a similar problem although it is closely related to the strain LEI and for the latter our primers managed to amplify this part of the SufDSU gene. Knowing that the diversity of the genus *Monocercomonoides* is high (Treitli et al., 2018) and the fact that we used only limited set of sequences for design of the primers we think that improved sampling of SufDSU sequences may help to design better primers which could in the future would amplify part of this gene from other *Monocercomonoides* strains.

We obtained five sequences of SufSU part of SufDSU gene and using phylogenetic analysis we showed that these sequences are truly oxymonad in origin as they group together with other sequences from oxymonads with high bootstrap support. However, we could not pinpoint the bacterial donor of the SUF system in oxymonads, even with our improved sampling of oxymonads. However, it has been shown that the bacterial donor of the SUF system cannot be determined even with multigene phylogeny and wider taxon sampling of Preaxostyla (Vacek et al., 2018).

For FISH analyses we used protocol from Zubáčová et al. (2011), but our initial FISH experiment showed high background and we needed to adapt the protocol. In our final protocol we increased the concetration of H_2O_2 from 1% to 3%. It seems that some of our cultures have high endogenous peroxidase activity, but it is not clear if the endogenous activity comes from bacteria or eukaryote, since the background was randomly scattered on the slides and not localized. Since our probes have sufficient length, we also increased the

washing temperature after hybridization from 42°C to 45°C. The probe concentration was also lowered from to 2 µl to 0,1 µl in the case of *Monocercomonoides mercovicenis* strains VAV1B and Marek2, *Monocercomonoides* sp. OEV and Mural1, and 0,2 µl in the case of *Monocercomonoides* sp. strain LEI. Finally, we reduced the time of amplification from 7 minutes to 5 minutes. All these changes helped to lower the background, however, the probes had a low hybridization efficiency of about 30%. The ploidy analyses using single copy genes using probes laleled with digoxigenin and detection with TSA system were also successfully used on other protists (Tůmová et al., 2016; Vazač et al., 2018; Zubáčová et al., 2011).

For the single copy gene FISH, we analyzed 50 nuclei for each strain. For all strains, we observed most of the time a single signal and rarely two signals (Table 16). The frequency of nuclei with two signals was usually around 5% which is expected when the culture is not synchronized and has a certain population of cells in G2 and S phases of the cell cycle. FISH against single copy genes strongly supported that all of our investigated strains are haploid. In another members of Metamonada, the haploid genome was reported in nine representatives of Parabasalia (e.g. *Trichomonas vaginalis*) (Zubáčová et al., 2011, 2008), while the members of diplomonadida like *Giardia intestinalis* (Morrison et al., 2007), *Spironucleus salmonicida* (Xu et al., 2014) or *Spironucleus barkhanus* (Roxström-Lindquist et al., 2010) have two similar diploid nuclei, which makes them tetraploid.

Various karyotype analyses among metamonads were performed using classical cytological methods with cells arrested in metaphaze by treatment with colchicine (Shen et al., 2011; Zubáčová et al., 2011, 2008).Unfortunately, in case of *Monocercomonoides* spp. this procedure was not working, so the analysis of karyotype were performed using FISH using probe against the telomeric repeats. We generated telomeric fragments using the protocol described by Ijdo (Ijdo et al., 1991) with a few modification. The telomeric DNA fragments generated by PCR were labelled using digoxygenin and vizualised by using DyLight 488 conjugated to anti-digoxygenin antibodies simular to the protocol used in Alverca et al. (Alverca et al., 2007). Even if successful telomeric detection using TSA-FISH was reported (Uzlíková et al., 2017; Vazač et al., 2018) we did not use signal amplification because the signals obtained without amplification were strong enough, moreover, with TSA, the signals would probably be too strong and we would not be able to distinguish between the individual signals.

For telomeric FISH we still kept the higher washing temperature of 45°C as in the protocol for single copy gene FISH. In order to reduce the human error when counting the

number of signals for each nucleus, we decided to count the number of signals automatically using ImageJ program. Since ImageJ marks all the signals which were counted, we also checked briefly each counted nucleus, to make sure that no signal was missed by the software. Our results suggest that the *Monocermonoides* sp. strains LEI, Mural1, ERYM1, OEV and *Monocermonoides acer* strain TENE79 have lower number of telomeric signals, the averages ranging from 9 to 17, which should correspond to approximately 4 to 9 chromosomes. These results are similar to the estimated karyotype of of ~7 chromosomes in *Monocermonoides exilis* strain PA203 (Karnkowska et al,. under review). These number of chromosomes are close to already known karyotypes of other Metamonada, namely *Trichomonas vaginalis* (6 chromosomes), *Trichomonas tenax* (6 chromosomes), *Tetratrichomonas gallinarum* (5 chromosomes), *Pentatrichomonas hominis* (6 chromosomes), *Tritrichomonas foetus* (5 chromosomes), *Tritrichomonas augusta* (5 chromosomes), *Monocercomonas colubrorum* (4 chromosomes), *Trichomitus batrachorum* (6 chromosomes) and *Hypotrichomonas acosta* (5 chromosomes) in haploid genomes (Zubáčová et al., 2011, 2008). For *Tritrichomonas foetus* and *Tritrichomonas suis* 10 chromosomes were obseeved durin metaphase.(Xu et al., 1998). In *Giardia intestinalis* who has two diploid nuclei in the trophozoite stage, making the cell tetraploid (Wampfler et al., 2014), the chromosome number was 10 with two sets of chromosomes in each nucleus (Shen et al., 2011). Interestingly the number of chromosomes slightly differ between *Giardia intestinalis* strains and even between the nuclei within the same cell (Tůmová et al., 2016).

In order to correlate the telomeric FISH and single copy gene FISH we also tried two colour FISH for simultaneous detection of single copy genes and telomeric repeats in one nucleus. The two-color FISH was successfully used on *Giardia intestinalis* (Tůmová et al., 2016). Unfortunatelly, due to endogenous biotin present in bacteria we could not use biotin for labeling of the probes. Using direct labeling with FITC dUTP for telomeric signals, the signal was not strong enough.

Monocercomonoides mercovicensis strain Marek2 and VAV1B were exceptional among our strains, because they showed a high number of telomeric signals with average 58 for strain Marek 2 and 107 for strain VAV1B. Intrestingly these two strains are classified to the same species (Treitli et al., 2018)**,** moreover, the amplified SufDSU part of the gene from the two strains is identical. All of these could suggest that these two strains could represent two different life stages. However, our single copy gene FISH suggests that both strains are haploid, which does not support this hypothesis. In addition, flow cytometry measurement

showed a really wide distribution of the DNA content in the strain VAV1B. One possible explanation for such observation is aneuploidy. This is, however, not supported by the single copy gene results, since cells with more than one signal were observed with similar frequency as in the case of other strains. Another reason for such a high number of telomeric signals can be caused by the presence of the telomeric-like repeats at internal sites of the chromosomes (intrachromosomal or interstitial telomerics equences, ITSs) (Aksenova et al., 2013; Nergadze et al., 2004; Ruiz-herrera et al., 2008). It is also possible that *Monocercomonoides mercovicensis* posses a population of minichromosomes, similarly to *Trypanosoma* sp. (Garside et al., 1994; Melville et al., 1998; Stanne et al., 2011). It is important to note, that our cultures are not clonal which can also cause the variation in DNA content. Flow cytometry measurement of the second strain Marek2 could help us to further shed light on the weird situation which we observe in this two strains. Unfortunatelly these measurements were not successful.

For flow cytometry analyses, we tried fixation of cells in 70% ethanol and various concentrations of formaldehyde, and in the end we decided that the optimal fixation condition is 1% formaldehyde. Because of our cultures are not axenic we always needed to filter the culturers before fixation, but even after these steps we still had plenty of bacteria in the sample. Before staining, we passed the samples through a 20 μm membrane to remove aggregates which can clog the flow cytometer. In the initial experiments the nuclei were stained with the Hoechst 33342 which was used also by Zubáčová et al. (2008), but this was not working very well in case of *Monocercomonoides* strains and we obtained better results using DAPI staining. For the calculation of the DNA content we needed a reference with the know DNA content. For this we used *Monocercomonoides exilis*, where we know that the haploid genome size is 82Mbp. This strain was always measured before each investigated strain to avoid any instrument variation between experimental days (eg. laser instability). We also kept the same setting during the measurements. The results (Figure 18) show that *Monocercomonoides* sp. strains OEV and Mural1 have smaller DNA content (= haploid genome sizes), with 30 and 36 Mbp respectively. Even in the case of strain LEI the estimated genome size was estimated to be 42 Mbp, but only two measurements were performed. For *Monocercomonoides* sp. strain ERYM1, we were able to measure DNA content only once due to the difficulty to culture this particular strain in larger volumes which are needed for flow cytometry. But it seems that genome size is close to *Monocermonoides exilis*, with a DNA content of approximately 69Mbp. In the case of TENE79 strain, we performed two replicates,

both suggesting larger genom size of about 106Mbp. But the largest DNA content appears to be in VAV1B strain, with the estimated genome size 129 Mbp.

Genomes of all *Monocercomonoides*strains are generally smaller when compared to the genomes of parabasalids like *Trichomonas vaginalis* (160 Mbp), *Trichomonas tenax* (133 Mbp), *Tetratrichomonas gallinarum* (86 Mbp), *Pentatrichomonas hominis* (94 Mbp), *Tritrichomonas foetus* (177 Mbp), *Tritrichomonas augusta* (165 Mbp), *Monocercomonas colubrorum* (114 Mbp), *Trichomitus batrachorum* (125 Mbp) and *Hypotrichomonas acosta* (114 Mbp) (Zubáčová et al., 2008). On the other hand, they are bigger than *Kipferlia bialata* with 51 Mbp (Tanifuji et al., 2018), *Giardia intestinalis* (11,7 Mbp) (Morrison et al., 2007) or Spironucleus *salmonicida* (12,9 Mbp) (Xu et al., 2014).

We also observed a wide variation of the DNA content in *Monocercomonoides mercovicensis.* A similar situation was found within various isolates of *Trypanosoma brucei gambiense, T. b. rodensiense and T. b. brucei*. The highest DNA content was observed in *T. b. brucei* and the lowest in *T. b. gambienese*, and it was suggested that the reduction of genome size may be caused by the depletion of minichromosomes (Kanmogne et al., 1997). This large range of DNA content among species was also observed for *Micrasterias* species. Interestingly, high variability in DNA content was also detected among different strains belonging to a single species (Poulíčková et al., 2014).

In the study of Zubáčová (Zubáčová et al., 2008) focused on genome sizes and karyotypes of various parabasalids positive correlation between DNA content and the cell and nucleus size was found. This corresponds with the hypothesis of Skeletal DNA, which claims that nuclear volumes are determined primarily by the DNA amounts (Cavalier-Smith, 2005). A strong correlation between the absolute nuclear DNA content and the cell size was also reported within genus *Micrasterias* (Poulíčková et al., 2014). Although not statistically analysed, *Monocercomonoides* strains with larger cells and nuclei (Tretli et al. 2018, Table 2) tend to have larger genome sizes. Exception represents *Monocercomonoides acer* strain TENE79, however, the measurement of DNA content for this strain was not made in in three replicates.

7. Summary

- Based on the FISH analyses and flow cytometry measurements, the *Monocermonoides* sp. strains OEV, LEI, Mural1, ERYM1 and *Monocermonoides acer* strain TENE 79 appears to be haploid with the number of chromosomes ranging between 4 and 9. The haploid genome sizes of these strains are ~ 106 Mbp in the case of *Monocermonoides acer* strain TENE79 and 30 to 69 Mbp in the case of the other strains.

- *Monocercomonoides mercovicensis* strains Marek2 and VAV1B represent exceptions. They both have much higher number of telomeric signals, average 58 signals for the strain Marek2 and 107 for the strain VAV1B. Still, single copy gene FISH suggests that both strains are haploid. Flow cytometry measurements showed a really wide distribution of the DNA content in strain VAV1B with the average haploid genome size 129 Mbp.

8. References

Akao, K., Minezawa, T., Yamamoto, N., Okamura, T., Inoue, T., Yamatsuta, K., Uozu, S., Goto, Y., Hayashi, M., Isogai, S., Kondo, M., Imaizumi, K., 2018. Flow cytometric analysis of lymphocyte profiles in mediastinal lymphadenopathy of sarcoidosis. PLoS One 13, e0206972.

Aksenova, A.Y., Greenwell, P.W., Dominska, M., Shishkin, A.A., Kim, J.C., Petes, T.D., Mirkin, S.M., 2013. Genome rearrangements caused by interstitial telomeric sequences in yeast. Proc. Natl. Acad. Sci. U. S. A. 110, 19866–19871. https://doi.org/10.1073/pnas.1319313110/-/DCSupplemental.www.pnas.org/cgi/doi/10.1073/pnas.1319313110

Alverca, E., Cuadrado, A., Jouve, N., Franca, S., Moreno Díaz de la Espina, S., 2007. Telomeric DNA localization on dinoflagellate chromosomes : structural and evolutionary implications. Cytogenet. Genome Res. 116, 224–231. https://doi.org/10.1159/000098191

Amann, R., Fuchs, B.M., Behrens, S., 2001. The identification of microorganisms by fluorescence *in situ* hybridisation. Curr. Opin. Biotechnol. 12, 231–236. https://doi.org/10.1016/S0958-1669(00)00204-4

Bakke, A.C., 2001. The Principles of Flow Cytometry. Lab. Med. 32, 207–211. https://doi.org/10.1007/s004410000193

Bauman, J.G., Wiegant, J., Borst, P., van Duijn, P., 1980. A new method for fluorescence microscopical localization of specific DNA sequences by in situ hybridization of fluorochromelabelled RNA. Exp. Cell Res. 128, 485–490.

Becker, A., Meister, A., Wilhelm, C., 2002. Flow cytometric discrimination of various phycobilin-containing phytoplankton groups in a hypertrophic reservoir. Cytometry 48, 45–57. https://doi.org/10.1002/cyto.10104

Bertani, G., 1951. Studies on lysogenesis. I. The mode of phage liberation by lysogenic Escherichia coli. J. Bacteriol. 62, 293–300.

Betters, D.M., 2015. Use of Flow Cytometry in Clinical Practice. J. Adv. Pract. Oncol. 6, 435–440. https://doi.org/10.6004/jadpro.2015.6.5.4

Brown, M., Wittwer, C., 2000. Flow Cytometry: Principles and Clinical Applications in Hematology. Clin. Chem. 46, 1221–1229.

Brugerolle, G., König, H., 1997. Ultrastructure and organization of the cytoskeleton *Oxymonas*, an intestinal flagellate of termites. J. Eukaryot. Microbiol. 44, 305–313. https://doi.org/10.1111/j.1550-7408.1997.tb05671.x

Brugerolle, G., Silva-Neto, I.D., Pellens, R., Grandcolas, P., 2003. Electron microscopic identification of the intestinal protozoan flagellates of the xylophagous cockroach *Parasphaeria boleiriana* from Brazil. Parasitol. Res. 90, 249–256. https://doi.org/10.1007/s00436-003-0832-7

Carabajal Paladino, L.Z., Nguyen, P., Šíchová, J., Marec, F., 2014. Mapping of single-copy genes by TSA-FISH in the codling moth, *Cydia pomonella*. BMC Genet. 15, S15. https://doi.org/10.1186/1471-2156-15-S2-S15

Carpenter, K.J., Horak, A., Chow, L., Keeling, P.J., 2011. Symbiosis, morphology, and phylogeny of hoplonymphidae (Parabasalia) of the wood-feeding roach *Cryptocercus punctulatus*. J. Eukaryot. Microbiol. 58, 426–436. https://doi.org/10.1111/j.1550-7408.2011.00564.x

Cavalier-Smith, T., 2005. Economy, speed and size matter: Evolutionary forces driving nuclear genome miniaturization and expansion. Ann. Bot. 95, 147–175. https://doi.org/10.1093/aob/mci010

Chen, A.Y., Chen, A., 2013. Fluorescence *In Situ* Hybridization. J. Invest. Dermatol. 133, e8. https://doi.org/10.1038/jid.2013.120

Chia, W.N., Lee, Y.Q., Tan, K.S.W., 2017. Imaging flow cytometry for the screening of compounds that disrupt the *Plasmodium falciparum* digestive vacuole. Methods 112, 211–220. https://doi.org/10.1016/j.ymeth.2016.07.002

Clark, M., 2002. In Situ Hybridization: Laboratory Companion. WILEY-VCH Verlag GmbH & Co, Weinheim.

Connolly, B.A.L., Jones, T.L., Ph, D., 2002. Hybridization Buffers I : Comparison of Formamide vs . Aqueous Hybridization Solutions.

Conrad, M., Zubacova, Z., Dunn, L.A., Upcroft, J., Sullivan, S.A., Tachezy, J., Carlton, J.M., 2011. Microsatellite polymorphism in the sexually transmitted human pathogen *Trichomonas vaginalis* indicates a genetically diverse parasite. Mol. Biochem. Parasitol. 175, 30–38. https://doi.org/10.1016/j.molbiopara.2010.08.006

Criscuolo, A., Gribaldo, S., 2010. BMGE (Block Mapping and Gathering with Entropy): a new software for selection of phylogenetic informative regions from multiple sequence alignments. BMC Evol. Biol. 10, 210.

Cui, C., Shu, W., Li, P., 2016. Fluorescence *In situ* Hybridization: Cell-Based Genetic Diagnostic and Research Applications. Front. Cell Dev. Biol. 4, 89. https://doi.org/10.3389/fcell.2016.00089

Dacks, J.B., Silberman, J.D., Simpson, A.G.B., Moriya, S., Kudo, T., Ohkuma, M., Redfield, R.J., 2001. Oxymonads are closely related to the excavate taxon *Trimastix*. Mol. Biol. Evol. 18, 1034–1044. https://doi.org/10.1093/oxfordjournals.molbev.a003875

Dapena, C., Bravo, I., Cuadrado, A., Figueroa, I.R., 2015. Nuclear and Cell Morphological Changes during the Cell Cycle and Growth of the Toxic Dinoflagellate *Alexandrium minutum*. Protist 166, 146–160. https://doi.org/10.1016/j.protis.2015.01.001

Darzynkiewicz, Z., Huang, X., Zhao, H., 2017. Analysis of Cellular DNA Content by Flow Cytometry DNA Content. Curr. Opin. Immunol. 119, 5.7.1–5.7.20. https://doi.org/10.1002/cpim.36

Dekel, E., Rivkin, A., Heidenreich, M., Nadav, Y., Ofir-Birin, Y., Porat, Z., Regev-Rudzki, N., 2017. Identification and classification of the malaria parasite blood developmental stages, using imaging flow cytometry. Methods 112, 157–166. https://doi.org/10.1016/j.ymeth.2016.06.021

der Strate, B. van, Longdin, R., Geerlings, M., Bachmayer, N., Cavallin, M., Litwin, V., Patel, M., Passe-Coutrin, W., Schoelch, C., Companjen, A., Fjording, M.S., 2017. Best practices in performing flow cytometry in a regulated environment: feedback from experience within the European Bioanalysis Forum. Bioanalysis 9, 1253–1264. https://doi.org/10.4155/bio-2017-0093

Diamond, L.S., 1982. A New Liquid Medium for Xenic Cultivation of Entamoeba histolytica and Other

Lumen- Dwelling Protozoa Author (s): Louis S . Diamond Source : The Journal of Parasitology , Vol . 68 , No . 5 (Oct ., 1982), pp . 958-959 Published by : Allen Press on beha. J. Parasitol. 68, 958–959.

Dolezel, J., Bartos, J., Voglmayr, H., Greilhuber, J., 2003. Nuclear DNA content and genome size of trout and human. Cytom. Part A 51A, 127–128. https://doi.org/10.1002/cyto.a.10013

Dolezel, J., Binarova, P., Lucretti, S., 1989. Analysis of Nuclear DNA content in plant cells by Flow Cytometry. Biol. Plant. 31, 113–120. https://doi.org/10.1007/BF02907241

Dolezel, J., Sgorbati, S., Lucretti, S., 1992. Comparison of three DNA fluorochromes for flow cytometric estimation of nuclear DNA content in plants. Physiol. Plant. 85, 625–631.

Erkes, D.A., Selvan, S.R., 2014. Hapten-induced contact hypersensitivity, autoimmune reactions, and tumor regression: Plausibility of mediating antitumor immunity. J. Immunol. Res. 2014, 28 pages. https://doi.org/10.1155/2014/175265

Feinberg, A.P., Vogelstein, B., 1983. This Week's Citation Classic DNA Labeling by Random Priming. Anal. Chem. 132, 6–13.

Fleck, R.A., Pickup, R.W., Day, J.G., Benson, E.E., 2006. Characterisation of cryoinjury in *Euglena gracilis* using flow-cytometry and cryomicroscopy. Cryobiology 52, 261–268. https://doi.org/10.1016/j.cryobiol.2005.12.003

Fulnečková, J., Ševčíková, T., Fajkus, J., Lukešová, A., Lukeš, M., Vlček, Č., Lang, B.F., Kim, E., Eliáš, M., Sýkorová, E., 2013. A broad phylogenetic survey unveils the diversity and evolution of telomeres in eukaryotes. Genome Biol. Evol. 5, 468–483. https://doi.org/10.1093/gbe/evt019

Garside, L., Bailey, M., Gibson, W., 1994. DNA content and molecular karyotype of trypanosomes of the subgenus *Nannomonas*. Acta Trop. 57, 21–28.

Giovannoni, S.J., DeLong, E.F., Olsen, G.J., Pace, N.R., 1988. Phylogenetic group-specific oligonucleotide probes for identification of single microbial cells. J. Bacteriol. 170, 720–726.

Hampl, V., 2017. Preaxostyla, in: Archibald, J.M., Simpson, A.G.B., Slamovits, C.H. (Eds.), Handbook of the Protist Second Edition. Springer International Publishing, pp. 1139–1175. https://doi.org/10.1007/978-3-319-28149-0

Hampl, V., Horner, D.S., Dyal, P., Kulda, J., Flegr, J., Foster, P.G., Embley, T.M., 2005. Inference of the phylogenetic position of oxymonads based on nine genes: Support for metamonada and Excavata. Mol. Biol. Evol. 22, 2508–2518. https://doi.org/10.1093/molbev/msi245

Haridas, V., Ranjbar, S., Vorobjev, I.A., Goldfeld, A.E., Barteneva, N.S., 2017. Imaging flow cytometry analysis of intracellular pathogens. Methods 112, 91–104. https://doi.org/10.1016/j.ymeth.2016.09.007

Hart, S.M., Basu, C., 2009. Optimization of a digoxigenin-based immunoassay system for gene detection in *Arabidopsis thaliana*. J. Biomol. Tech. 20, 96–100.

Hepperger, C., Otten, S., von Hase, J., Dietzel, S., 2007. Preservation of large-scale chromatin structure in FISH experiments. Chromosoma 116, 117–133. https://doi.org/10.1007/s00412-006-0084-2

Hongoh, Y., Sato, T., Noda, S., Ui, S., Kudo, T., Ohkuma, M., 2007. Candidatus *Symbiothrix*

dinenymphae: Bristle-like Bacteroidales ectosymbionts of termite gut protists. Environ. Microbiol. 9, 2631–2635. https://doi.org/10.1111/j.1462-2920.2007.01365.x

Hu, L., Ru, K., Zhang, L., Huang, Y., Zhu, X., Liu, H., Zetterberg, A., Cheng, T., Miao, W., 2014. Fluorescence in situ hybridization (FISH): An increasingly demanded tool for biomarker research and personalized medicine. Biomark. Res. 2, 1–13. https://doi.org/10.1186/2050-7771-2-3

Iida, T., Ohkuma, M., Ohtoko, K., Kudo, T., 2000. Symbiotic spirochetes in the termite hindgut: Phylogenetic identification of ectosymbiotic spirochetes of oxymonad protists. FEMS Microbiol. Ecol. 34, 17–26. https://doi.org/10.1016/S0168-6496(00)00070-2

Ijdo, J.W., Wells, R.A., Baldini, A., Reeders, S.T., 1991. Improved telomere detection using a telomere repeat probe (TTAGGG) n generated by PCR 19, 4780.

Kanmogne, G.D., Bailey, M., Gibson, W.C., 1997. Wide variation in DNA content among isolates of *Trypanosoma brucei* ssp . Acta Trop. 63, 75–87.

Kapuscinski, J., 1995. DAPI: A DMA-Specific fluorescent probe. Biotech. Histochem. 70, 220–233. https://doi.org/10.3109/10520299509108199

Karnkowska, A., Vacek, V., Zubáčová, Z., Treitli, S.C., Petrželková, R., Eme, L., Novák, L., Žárský, V., Barlow, L.D., Herman, E.K., Soukal, P., Hroudová, M., Doležal, P., Stairs, C.W., Roger, A.J., Eliáš, M., Dacks, J.B., Vlček, Č., Hampl, V., 2016. A eukaryote without a mitochondrial organelle. Curr. Biol. 26, 1274–1284. https://doi.org/10.1016/j.cub.2016.03.053

Katoh, K., Standley, D.M., 2013. MAFFT Multiple Sequence Alignment Software Version 7 : Improvements in Performance and Usability. Mol. Biol. Evol. 30, 772–780. https://doi.org/10.1093/molbev/mst010

Kawakami, S., Kubota, K., Imachi, H., Yamaguchi, T., Harada, H., Ohashi, A., 2010. Detection of Single Copy Genes by Two-Pass Tyramide Signal Amplification Fluorescence *in situ* Hybridization (Two-Pass TSA-FISH) with Single Oligonucleotide Probes. Microbes Environ. 25, 15–21. https://doi.org/10.1264/jsme2.ME09180

Keeling, P.J., Leander, B.S., 2003. Characterisation of a Non-canonical genetic code in the oxymonad *Streblomastix strix*. J. Mol. Biol. 326, 1337–1349. https://doi.org/10.1016/S0022-2836(03)00057-3

Khrustaleva, L.I., Kik, C., 2001. Localization of single-copy T-DNA insertion in transgenic shallots (Allium cepa) by using ultra-sensitive FISH with tyramide signal amplification. Plant J. 25, 699–707. https://doi.org/10.1046/j.1365-313X.2001.00995.x

Kislauskis, E.H., Li, Z., Singer, R.H., Taneja, K.L., 1993. Isoform-specific 3'-untranslated sequences sort alpha-cardiac and beta-cytoplasmic actin messenger RNAs to different cytoplasmic compartments. J. Cell Biol. 123, 165–172.

Krishnamurthy, R., Sultana, T., 1976. *Tubulimonoides gryllotalpae* n.g., n.sp. (Mastigophora: Oxymonadida) from the cricket in India. Proc. Indian Acad. Sci. 84 B, 137–140.

Langer, P.R., Waldrop, A.A., Ward, D.C., 1981. Enzymatic synthesis of biotin-labeled polynucleotides: novel nucleic acid affinity probes. Proc. Natl. Acad. Sci. U. S. A. 78, 6633–6637.

Leander, B.S., Keeling, P.J., 2004. Symbiotic innovation in the oxymonad *Streblomastix strix*. J. Eukaryot. Microbiol. 51, 291–300. https://doi.org/10.1111/j.1550-7408.2004.tb00569.x

Levsky, J.M., Singer, R.H., 2003. Fluorescence in situ hybridization: past, present and future. J. Cell Sci. 116, 2833–2838. https://doi.org/10.1242/jcs.00633

M. Kuwajima, 2011. Cross-linking fixatives : What they are , what they do , and why we use them. Kristen Harris Lab USA.

Manuelidis, L., Langer-Safer, P.R., Ward, D.C., 1982. High-resolution mapping of satellite DNA using biotin-labeled DNA probes. J. Cell Biol. 95, 619–625.

Mcintosh, R.J., 1973. The axostyle of *Saccinobaculus*: II. Motion of the microtubule bundle and a structural comparison of straight and bent axostyles. J. Cell Biol. 56, 324–339. https://doi.org/10.1083/jcb.56.2.324

McIntosh, R.J., Ogata, E.S., Landis, S.C., 1973. The axostyle of *Saccinobaculus*: I. Structure of the organism and its microtubule bundle. J. Cell Biol. 56, 304–323. https://doi.org/10.1083/jcb.56.2.304

Melville, S.E., Leech, V., Gerrard, C.S., Tait, A., Blackwell, J.M., 1998. The molecular karyotype of the megabase chromosomes of *Trypanosoma brucei* and the assignment of chromosome markers. Mol. Biochem. Parasitol. 94, 155–173.

Moriya, S., Dacks, J.B., Takagi, A., Noda, S., Ohkuma, M., Doolittle, W.F., Kudo, T., 2003. Molecular Phylogeny of Three Oxymonad Genera: *Pyrsonympha*, *Dinenympha* and *Oxymonas*. J. Eukaryot. Microbiol. 50, 190–197.

Moriya, S., Ohkuma, M., Kudo, T., 1998. Phylogenetic position of symbiotic protist *Dinemympha exilis* in the hindgut of the termite *Reticulitermes speratus* inferred from the protein phylogeny of elongation factor 1α. Gene 210, 221–227. https://doi.org/10.1016/S0378-1119(98)00078-X

Morrison, H.G., Mcarthur, A.G., Gillin, F.D., Aley, S.B., Adam, R.D., Olsen, G.J., Best, A.A., Cande, W.Z., Chen, F., Cipriano, M.J., Davids, B.J., Dawson, S.C., Elmendorf, H.G., Hehl, A.B., Holder, M.E., Huse, S.M., Kim, U.U., Lasek-nesselquist, E., Manning, G., Nigam, A., Nixon, J.E.J., Palm, D., Passamaneck, N.E., Prabhu, A., Reich, C.I., Reiner, D.S., Samuelson, J., Svard, S.G., Sogin, M.L., 2007. Genomic Minimalism in the Early Diverging Intestinal Parasite *Giardia lamblia*. Science (80-.). 317, 1921–1927.

Morrison, L.E., Ramakrishnan, R., Ruffalo, T.M., Wilber, K.A., 2002. Labeling Fluorescence In Situ Hybridization Probes for Genomic Targets, in: Fan, Y.S. (Ed.), Molecular Cytogenetics. Humana Press.

Moter, A., Göbel, U.B., 2000. Fluorescence in situ hybridization (FISH) for direct visualization of microorganisms. J. Microbiol. Methods 41, 85–112. https://doi.org/10.1016/S0167-7012(00)00152-4

Naves, L.L., da Silva, M.V., Fajardo, E.F., da Silva, R.B., De Vito, F.B., Rodrigues, V., Lages-Silva, E., Ramírez, L.E., Pedrosa, A.L., 2017. DNA content analysis allows discrimination between *Trypanosoma cruzi* and *Trypanosoma rangeli*. PLoS One 12, e0189907.

Nedbal, J., Hobson, P.S., Fear, D.J., Heintzmann, R., Gould, H.J., 2012. Comprehensive FISH Probe Design Tool Applied to Imaging Human Immunoglobulin Class Switch Recombination. PLoS One 7, e51675. https://doi.org/10.1371/journal.pone.0051675

Nergadze, S.G., Rocchi, M., Azzalin, C.M., Mondello, C., Giulotto, E., 2004. Insertion of telomeric repeats at intrachromosomal break sites during primate evolution. Genome Res. 14, 1704–

1710. https://doi.org/10.1101/gr.2778904

Noda, S., Inoue, T., Hongoh, Y., Kawai, M., Nalepa, C.A., Vongkaluang, C., Kudo, T., Ohkuma, M., 2006. Identification and characterization of ectosymbionts of distinct lineages in *Bacteroidales* attached to flagellated protists in the gut of termites and a wood-feeding cockroach. Environ. Microbiol. 8, 11–20. https://doi.org/10.1111/j.1462-2920.2005.00860.x

Noda, S., Ohkuma, M., Yamada, A., Hongoh, Y., Kudo, T., 2003. Phylogenetic position and in situ identification of ectosymbiotic spirochetes on protists in the termite gut. Appl. Environ. Microbiol. 69, 625–633. https://doi.org/10.1128/AEM.69.1.625-633.2003

Olefeld, J.L., Majda, S., Albach, D.C., Marks, S., Boenigk, J., 2018. Genome size of chrysophytes varies with cell size and nutritional mode. Org. Divers. Evol. 18, 163–173. https://doi.org/10.1007/s13127-018-0365-7

Olson, R.J., Frankel, S.L., Chisholm, S.W., Shapiro, H.M., 1983. An inexpensive flow cytometer for the analysis of fluorescence signals in phytoplankton: Chlorophyll and DNA distributions. J. Exp. Mar. Bio. Ecol. 68, 129–144. https://doi.org/10.1016/0022-0981(83)90155-7

Pérez, R., De Bustos, A., Jouve, N., Cuadrado, Á., 2009. Localization of rad50, a single-copy gene, on group 5 chromosomes of wheat, using a FISH protocol employing tyramide for signal amplification (Tyr-FISH). Cytogenet. Genome Res. 125, 321–328. https://doi.org/10.1159/000235938

Poulíčková, A., Mazalová, P., Vašut, R.J., Šarhanová, P., Neustupa, J., Škaloud, P., 2014. DNA content variation and its significance in the evolution of the genus Micrasterias (desmidiales, streptophyta). PLoS One 9, e92399. https://doi.org/10.1371/journal.pone.0086247

Raap, A.K., 1998. Advances in fluorescence in situ hybridization. Mutat. Res. 400, 287–298. https://doi.org/10.1016/S0027-5107(98)00029-3

Radek, R., 1994. *Monocercomonoides* termitis n. sp., an Oxymonad from the Lower Termite *Kalotermes sinaicus*. Arch. fur Protistenkd. 144, 373–382. https://doi.org/10.1016/S0003-9365(11)80240-X

Radek, R., Strassert, J.F.H., Krüger, J., Meuser, K., Scheffrahn, R.H., Brune, A., 2014. Phylogeny and Ultrastructure of Oxymonas jouteli, a Rostellum-free Species, and Opisthomitus longiflagellatus sp. nov., Oxymonadid Flagellates from the Gut of Neotermes jouteli. Protist 165, 384–399. https://doi.org/10.1016/j.protis.2014.04.003

Rae Rho, I., Hwang, Y.J., Lee, H. Il, Lee, C.H., Lim, K.B., 2012. Karyotype analysis using FISH (fluorescence in situ hybridization) in *Fragaria*. Sci. Hortic. (Amsterdam). 136, 95–100. https://doi.org/10.1016/j.scienta.2011.12.025

Rahman, M., 2014. Introduction to Flow Cytometry, Rahman, Mi. ed. AbD Serotec.

Ratan, Z.A., Zaman, S. Bin, Mehta, V., Haidere, M.F., Runa, N.J., Akter, N., 2017. Application of Fluorescence In Situ Hybridization (FISH) Technique for the Detection of Genetic Aberration in Medical Science Mechanism of FISH. Cureus 9, e1325. https://doi.org/10.7759/cureus.1325

Rieder, F., Kessler, S.P., West, G.A., Bhilocha, S., Motte, C. De, Sadler, T.M., Gopalan, B., Stylianou, E., Fiocchi, C., 2011. Inflammation-Induced Endothelial-to-Mesenchymal Transition: A Novel Mechanism of Intestinal Fibrosis. Am. J. Pathol. 179, 2660–2673. https://doi.org/10.1016/j.ajpath.2011.07.042

Rother, A., Radek, R., Hausmann, K., 1999. Characterization of surface structures covering termite flagellates of the family oxymonadidae and ultrastructure of two oxymonad species, *Microrhopalodina multinudeata* and *Oxymonas* sp. Eur. J. Protistol. 35, 1–16. https://doi.org/10.1016/S0932-4739(99)80018-2

Roxström-Lindquist, K., Jerlström-Hultqvist, J., Jørgensen, A., Troell, K., Svärd, S.G., Andersson, J.O., 2010. Large genomic differences between the morphologically indistinguishable diplomonads Spironucleus barkhanus and Spironucleus salmonicida. BMC Genomics 11. https://doi.org/10.1186/1471-2164-11-258

Ruiz-herrera, A., Nergadze, S.G., Santagostino, M., Giulotto, E., 2008. Telomeric repeats far from the ends: mechanisms of origin and role in evolution. Cytogenet. Genome Res. 122, 219–228. https://doi.org/10.1159/000167807

Sakai, M., Okumura, S.I., Onuma, K., Senbokuya, H., Yamamori, K., 2007. Identification of a telomere sequence type in three sponge species (Porifera) by fluorescence *in situ* hybridization analysis. Fish. Sci. 73, 77–80. https://doi.org/10.1111/j.1444-2906.2007.01304.x

Schriml, L.M., Padilla-Nash, H.M., Coleman, A., Moen, P., Nash, W.G., Menninger, J., Jones, G., Ried, T., Dean, M., 1999. Tyramide signal amplification (TSA)-FISH applied to mapping PCR-labeled probes less than 1 kb in size. Biotechniques 27, 608–613.

Schwarz-Finsterle, J., Stein, S., Großmann, C., Schmitt, E., Trakhtenbrot, L., Rechavi, G., Amariglio, N., Cremer, C., Hausmann, M., 2007. Comparison of triple helical COMBO-FISH and standard FISH by means of quantitative microscopic image analysis of abl/bcr positions in cell nuclei. J. Biochem. Biophys. Methods 70, 397–406. https://doi.org/10.1016/j.jbbm.2006.09.004

Shah, J., Mark, O., Weltman, H., Barcelo, N., Lo, W., Wronska, D., Kakkilaya, S., Rao, A., Bhat, S.T., Sinha, R., Omar, S., O'bare, P., Moro, M., Gilman, R.H., Harris, N., 2015. Fluorescence *In Situ* hybridization (FISH) assays for diagnosing malaria in endemic areas. PLoS One 10, e0136726. https://doi.org/10.1371/journal.pone.0136726

Sharpe, J., Ahlgren, U., Perry, P., Hill, B., Ross, A., Hecksher-Sørensen, J., Baldock, R., Davidson, D., 2002. Optical projection tomography as a tool for 3D microscopy and gene expression studies. Science 296, 541–545. https://doi.org/10.1126/science.1068206

Shen, H.E., Cao, L., Li, J., Tian, X.F., Yang, Z.H., Wang, Y., Tian, Y.N., Lu, S.Q., 2011. Visualization of chromosomes in the binucleate intestinal parasite *Giardia lamblia*. Parasitol. Res. 109, 1439–1445. https://doi.org/10.1007/s00436-011-2392-6

Shreder, K., 2000. Synthetic haptens as probes of antibody response and immunorecognition. Methods 20, 372–379. https://doi.org/10.1006/meth.1999.0929

Silva, G.S., Souza, M.M., de Melo, C.A.F., Urdampilleta, J.D., Forni-Martins, E.R., 2018. Identification and characterization of karyotype in *Passiflora* hybrids using FISH and GISH. BMC Genet. 19, 26. https://doi.org/10.1186/s12863-018-0612-0

Simpson, A.G.B., 2003. Cytoskeletal organization , phylogenetic affinities and systematics in the contentious taxon Excavata (Eukaryota). Int. J. Syst. Evol. Microbiol. 53, 1759–1777. https://doi.org/10.1099/ijs.0.02578-0

Simpson, A.G.B., Radek, R., Dacks, J.B., O'Kelly, C.J., 2002. How oxymonads lost their groove: An ultrastructural comparison of *Monocercomonoides* and excavate taxa. J. Eukaryot. Microbiol. 49, 239–248. https://doi.org/10.1111/j.1550-7408.2002.tb00529.x

Spear, R.N., Li, S., Nordheimb, E. V, Andrewsa, J.H., 1999. Quantitative imaging and statistical analysis of fluorescence in situ hybridization (FISH) of Aureobasidium pullulans. J. Microbiol. Methods 35, 101–110. https://doi.org/10.1016/s0167-7012(98)00100-6

Stamatakis, A., 2006. RAxML-VI-HPC: maximum likelihood-based phylogenetic analyses with thousands of taxa and mixed models Alexandros. Bioinformatics 22, 2688–2690. https://doi.org/10.1093/bioinformatics/btl446

Stanne, T.M., Kushwaha, M., Wand, M., Taylor, J.E., Rudenko, G., 2011. TbISWI Regulates Multiple Polymerase I (Pol I)-Transcribed Loci and Is Present at Pol II Transcription Boundaries in *Trypanosoma brucei*. Eukaryot. Cell 10, 964–976. https://doi.org/10.1128/EC.05048-11

Stingl, U., Radek, R., Yang, H., Brune, A., 2005. "*Endomicrobia*": Cytoplasmic Symbionts of Termite Gut Protozoa Form a Separate Phylum of Prokaryotes. Appl. Environ. Microbiol. 71, 1473–1479. https://doi.org/10.1128/AEM.71.3.1473

Tanifuji, G., Takabayashi, S., Kume, K., Takagi, M., Nakayama, T., Kamikawa, R., Inagaki, Y., Hashimoto, T., 2018. The draft genome of *Kipferlia bialata* reveals reductive genome evolution in fornicate parasites. PLoS One 13, e0194487.

Todd, R.T., Forche, A., Selmecki, A., 2017. Ploidy Variation in Fungi: Polyploidy, Aneuploidy, and Genome Evolution. Microbiol. Spectr. 5, FUNK-0051-2016. https://doi.org/10.1128/microbiolspec.FUNK-0051-2016.Ploidy

Trask, B.J., van den Engh, G.J., Elgershuizen, J.H.B.W., 1982. Analysis of phytoplankton by flow cytometry. Cytometry 2, 258–264. https://doi.org/10.1002/cyto.990020410

Treitli, S.C., Kotyk, M., Yubuki, N., Jirounková, E., Vlasáková, J., Smejkalová, P., Šípek, P., Čepička, I., Hampl, V., 2018. Molecular and Morphological Diversity of the Oxymonad Genera *Monocercomonoides* and *Blattamonas* gen. nov. Protist 169, 744–783. https://doi.org/10.1016/j.protis.2018.06.005

Tůmová, P., Uzlíková, M., Jurczyk, T., Nohýnková, E., 2016. Constitutive aneuploidy and genomic instability in the single-celled eukaryote Giardia intestinalis. Microbiologyopen 5, 560–574. https://doi.org/10.1002/mbo3.351

Uzlíková, M., Fulnečková, J., Weisz, F., Sýkorová, E., Nohýlková, E., Tůmová, P., 2017. Characterization of telomeres and telomerase from the single-celled eukaryote *Giardia intestinalis*. Mol. Biochem. Parasitol. 211, 31–38. https://doi.org/10.1016/j.molbiopara.2016.09.003

Vacek, V., Novák, L.V.F., Treitli, S.C., Táborský, P., Čepička, I., Kolísko, M., Keeling, P.J., Hampl, V., 2018. Fe–S Cluster Assembly in Oxymonads and Related Protists. Mol. Biol. Evol. 35, 2712–2718. https://doi.org/10.1093/molbev/msy168

Van De Corput, M.P.C., Dirks, R.W., Van de Rijke, F.M., Raap, A.K., 1998. Fluorescence in situ hybridization using horseradish peroxidase-labeled oligodeoxynucleotides and tyramide signal amplification for sensitive DNA and mRNA detection. Histochem Cell Biol. 110, 431–437. https://doi.org/10.1177/002215549804601105

Van Tine, B.A., Kappes, J.C., Banerjee, N.S., Knops, J., Lai, L., Steenbergen, R.D.M., Meijer, C.L.J.M., Snijders, P.J.F., Chatis, P., Broker, T.R., Moen, P.T., Chow, L.T., 2004. Clonal selection for transcriptionally active viral oncogenes during progression to cancer. J. Virol. 78, 11172–11186. https://doi.org/10.1006/jcis.1998.6054

Vazač, J., Füssy, Z., Hladová, I., Killi, S., Oborník, M., 2018. Ploidy and Number of Chromosomes in the Alveolate Alga *Chromera velia*. Protist 169, 53–63. https://doi.org/10.1016/j.protis.2017.12.001

Volpi, E. V., Bridger, J.M., 2008. FISH glossary: An overview of the fluorescence in situ hybridization technique. Biotechniques 45, 385–409. https://doi.org/10.2144/000112811

Wallner, G., Amann, R., Beisker, W., 1993. Optimizing Fluorescent In Situ Hybridization With rRNA-Targeted Oligonucleotide Probes for Flow Cytometric Identification of Microorganisms. Cytometry 14, 136–143.

Wampfler, P.B., Faso, C., Hehl, A.B., 2014. The Cre/loxP system in *Giardia lamblia*: genetic manipulations in a binucleate tetraploid protozoan. Int. J. Parasitol. 44, 497–506. https://doi.org/10.1016/j.ijpara.2014.03.008

Wang, C.-J.R., Harper, L., Cande, Y., 2006. High-Resolution Single-Copy Gene Fluorescence in Situ Hybridization and Its Use in the Construction of a Cytogenetic Map of Maize Chromosome 9. Plant Cell Online 18, 529–544. https://doi.org/10.1105/tpc.105.037838

Wiegant, J., Ried, T., Nederlof, P.M., van der Ploeg, M., Tanke, H.J., Raap, A.K., 1991. In situ hybridization with fluoresceinated DNA. Nucleic Acids Res. 19, 3237–3241.

Wilder, H.C., 1935. An Improved Technique for Silver Impregnation of Reticulum Fibers. Am. J. Pathol. 11, 817–820.

Xu, F., Jerlstrom-Hultqvist, J., Einarsson, E., Ástvaldsson, Á., Svard, S.G., Andersson, J.O., 2014. The Genome of *Spironucleus salmonicida* Highlights a Fish Pathogen Adapted to Fluctuating Environments. PLoS Genet. 10, e1004053. https://doi.org/10.1371/journal.pgen.1004053

Xu, W., Lun, Z., Gajadhar, A., 1998. Chromosome numbers of *Tritrichomonas foetus* and *Tritrichomonas suis*. Vet. Parasitol. 78, 247–251.

Yan, J., Zhang, J., Sun, K., Chang, D., Bai, S., Shen, Y., Huang, L., Zhang, J., Yhang, Y., Dong, Y., 2016. Ploidy Level and DNA Content of *Erianthus arundinaceus* as Determined by Flow Cytometry and the Association with Biological Characteristics. PLoS One 11, e0151948. https://doi.org/10.1371/journal.pone.0151948

Yang, H., Schmitt-Wagner, D., Stingl, U., Brune, A., 2005. Niche heterogeneity determines bacterial community structure in the termite gut (*Reticulitermes santonensis*). Environ. Microbiol. 7, 916–932. https://doi.org/10.1111/j.1462-2920.2005.00760.x

Yason, J.A., Tan, K.S.W., 2015. Seeing the whole elephant: Imaging flow cytometry reveals extensive morphological diversity within *Blastocystis* isolates. PLoS One 10, e0143974. https://doi.org/10.1371/journal.pone.0143974

Zhang, Q., Táborský, P., Silberman, J.D., Pánek, T., Čepička, I., Simpson, A.G.B., 2015. Marine Isolates of *Trimastix marina* Form a Plesiomorphic Deep-branching Lineage within Preaxostyla, Separate from Other Known Trimastigids (*Paratrimastix* n. gen.). Protist 166, 468–491. https://doi.org/10.1016/j.protis.2015.07.003

Zubáčová, Z., Cimbůrek, Z., Tachezy, J., 2008. Comparative analysis of trichomonad genome sizes and karyotypes. Mol. Biochem. Parasitol. 161, 49–54. https://doi.org/10.1016/j.molbiopara.2008.06.004

Zubáčová, Z., Krylov, V., Tachezy, J., 2011. Fluorescence *in situ* hybridization (FISH) mapping of single

copy genes on *Trichomonas vaginalis* chromosomes. Mol. Biochem. Parasitol. 176, 135–137. https://doi.org/10.1016/j.molbiopara.2010.12.011